Higgs of cold atoms and cavity

Wu-Ming Liu (刘伍明)

Institute of Physics, Chinese Academy of Sciences

(中国科学院物理所)

Email: wmliu@iphy.ac.cn

Supported by NSFC, MOST, CAS

Collaborators

Fei-Jie HUANG（黄飞杰）

Xiao-Lu YU（余小鲁）

Shang-Shun ZHANG（张尚舜）

Yi-Xiang YU（喻益湘）

Ren-Yuan LIAO（廖任远）

Jin-Wu YE（叶锦武）

Outline

1. Introduction
2. Higgs in cold atoms
3. Collective mode
4. Itinerant ferromagnetism
5. Tricritical point
6. Higgs in cavity
7. Summary

1. Introduction

Particle physics: Higgs boson

Condensed matter physics: superconductors, superfluids, magnet, semiconductor, nano-materials, etc.

Cold atoms: superfluid-Mott transition etc.

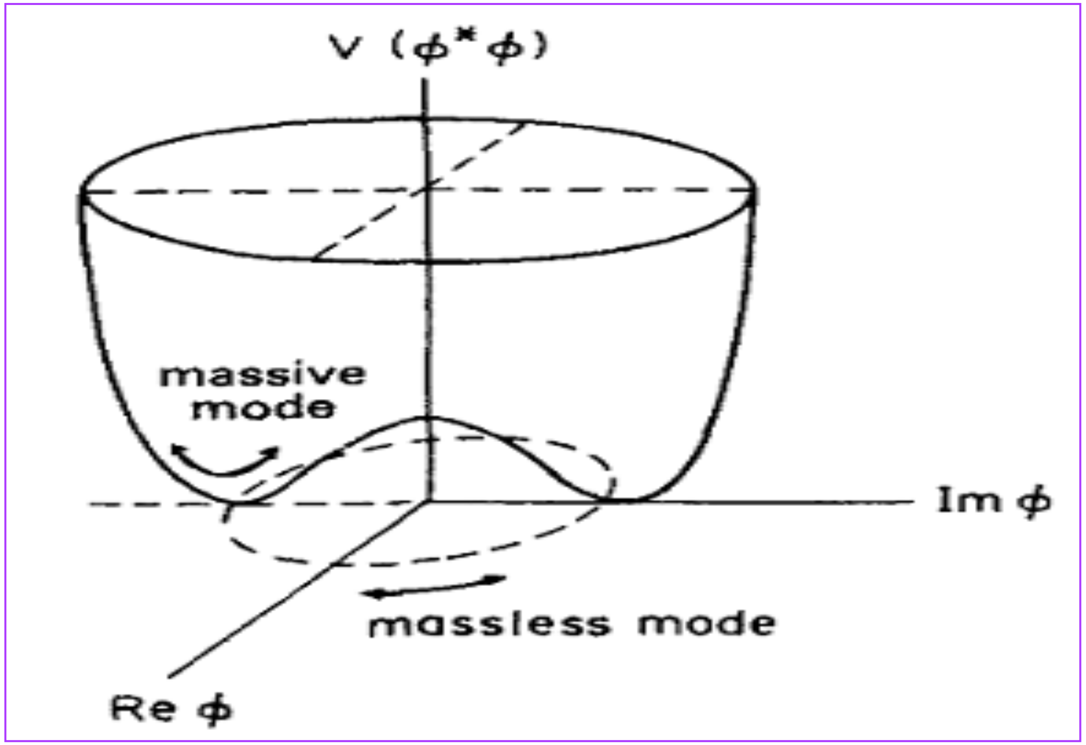

Non-Abelian gauge potential

$$F_{\mu\nu} = \partial_\mu A_\nu - \partial_\nu A_\mu - i\,\underline{g[A_\mu,\ A_\nu]}$$

$$A_\mu = A_\mu^i \sigma_i$$

Example $\quad A_\mu = A_0$

$$F_{\mu\nu} = F_{00} = -i\,g[A_0,\ A_0]$$

Higgs term

$$\boxed{\operatorname{Tr} F_{00} F_{00} = -g^2 \operatorname{Tr}[A_0,\ A_0][A_0,\ A_0]}$$

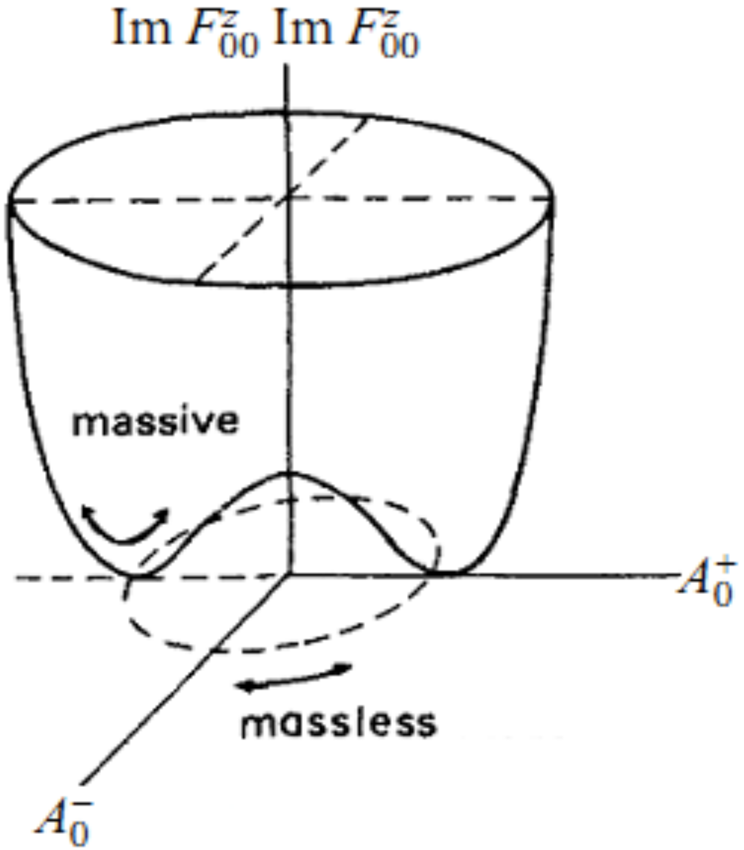

2. Higgs in cold atoms

Non-Abelian gauge potential

$$A_\mu = A^i_\mu \sigma_i \qquad F_{\mu\nu} = \partial_\mu A_\nu - \partial_\nu A_\mu - i\, \underline{g[A_\mu,\ A_\nu]}$$

Cold atoms : spin-orbit coupling   Nature **471**, 83 (2011)

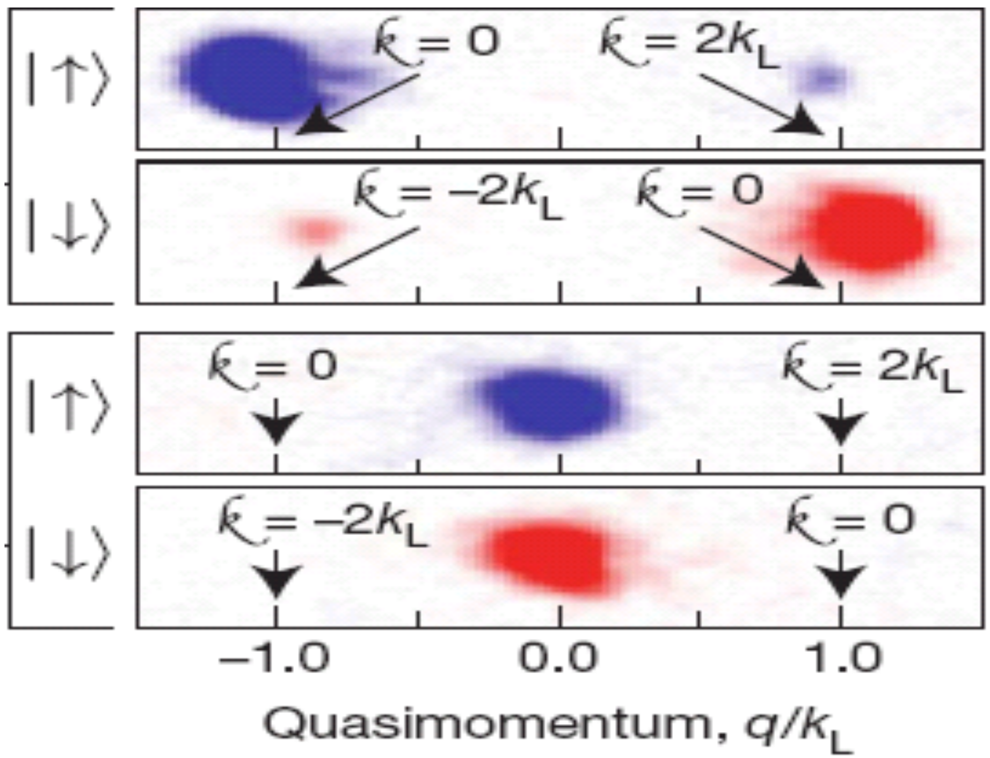

F.J. Huang, Q.H. Chen, W.M. Liu, Phys. Rev. A 89, 033624 (2014)

Cold atoms : SO coupling

$$\eta = p/2mc$$

$$g = \eta g_0, \quad g_0 = 1$$

$$H = (2m)^{-1}\left(\vec{p} + \underline{\vec{a}^i \sigma_i}\right)^2 = \eta p c + \underline{g A_0} + \text{const.}$$

Berry gauge potential

SO coupling $\Rightarrow$ $g A_0 = (2m)^{-1}\left(\vec{p}\cdot\vec{a}^i + \vec{a}^i\cdot\vec{p}\right)\sigma_i$

Effective gauge potential

$$\boxed{A_0 = \left(\vec{\gamma}\cdot\vec{a}^i + \vec{a}^i\cdot\vec{\gamma}\right)\sigma_i}$$

$$\vec{\gamma} = \vec{p}/p$$

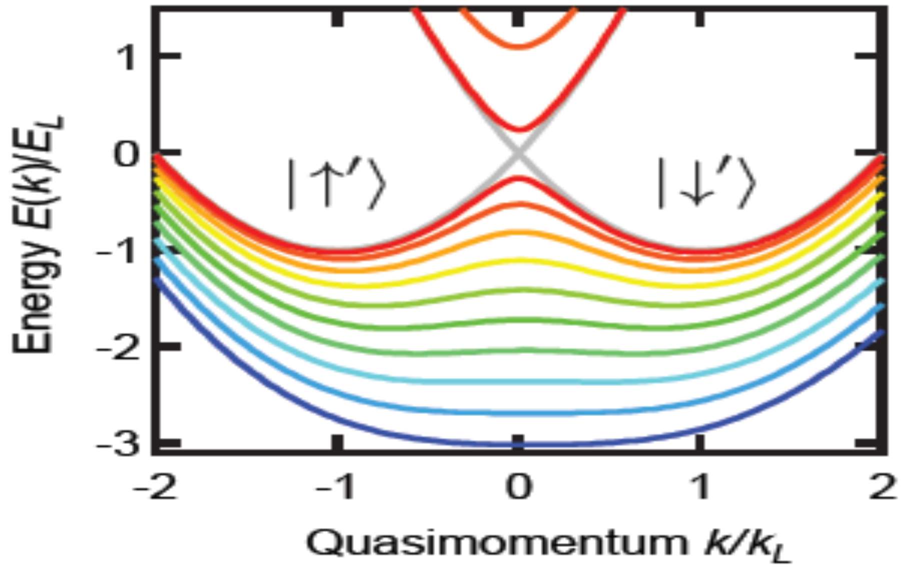

SO coupling in cold atoms

The relation between SO coupling and Higgs excitations in cold atoms

$$g A_0 = (2m)^{-1} \left(\vec{p} \cdot \vec{a}^i + \vec{a}^i \cdot \vec{p}\right) \sigma_i$$

$$H = \eta\, p\, c + \underline{g\, A_0}$$

The equation of motion of spin

$$i\, \partial_t \sigma = [\sigma,\ H] = [\sigma,\ \underline{A_0}]$$

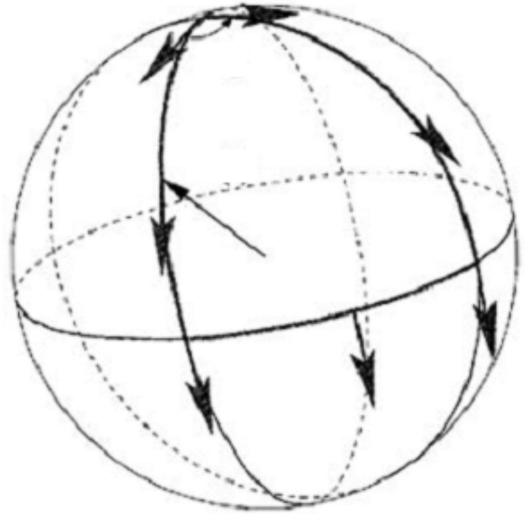

$$\nabla_0 = \partial_0 + [A_0,]\quad \partial_0 = i\, \partial_t$$

$$\boxed{\nabla_0 \sigma = 0}$$

Parallel transportation

Decomposition of gauge potential

$$B=[\sigma,\ \nabla_0\sigma]$$

$$A_0 = A + B$$

$$A = (\sigma \cdot A_0)\,\sigma + [\partial_0\sigma,\ \sigma]$$

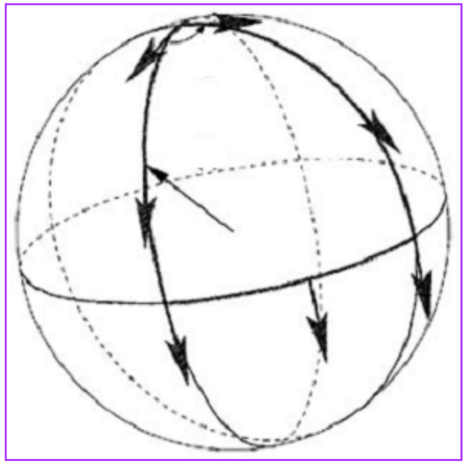

$\nabla_0\sigma=0 \Rightarrow A_0 = A$ SO coupling

$\boxed{\nabla_0\sigma\neq 0} \Rightarrow A_0 = A + B$ SO coupling + Higgs term

Higgs term

$$\boxed{\mathrm{Tr}\,F_{00}\,F_{00} = -g^2\,\mathrm{Tr}\,[B,\ B][B,\ B]}$$

The sphere surface of gauge potential

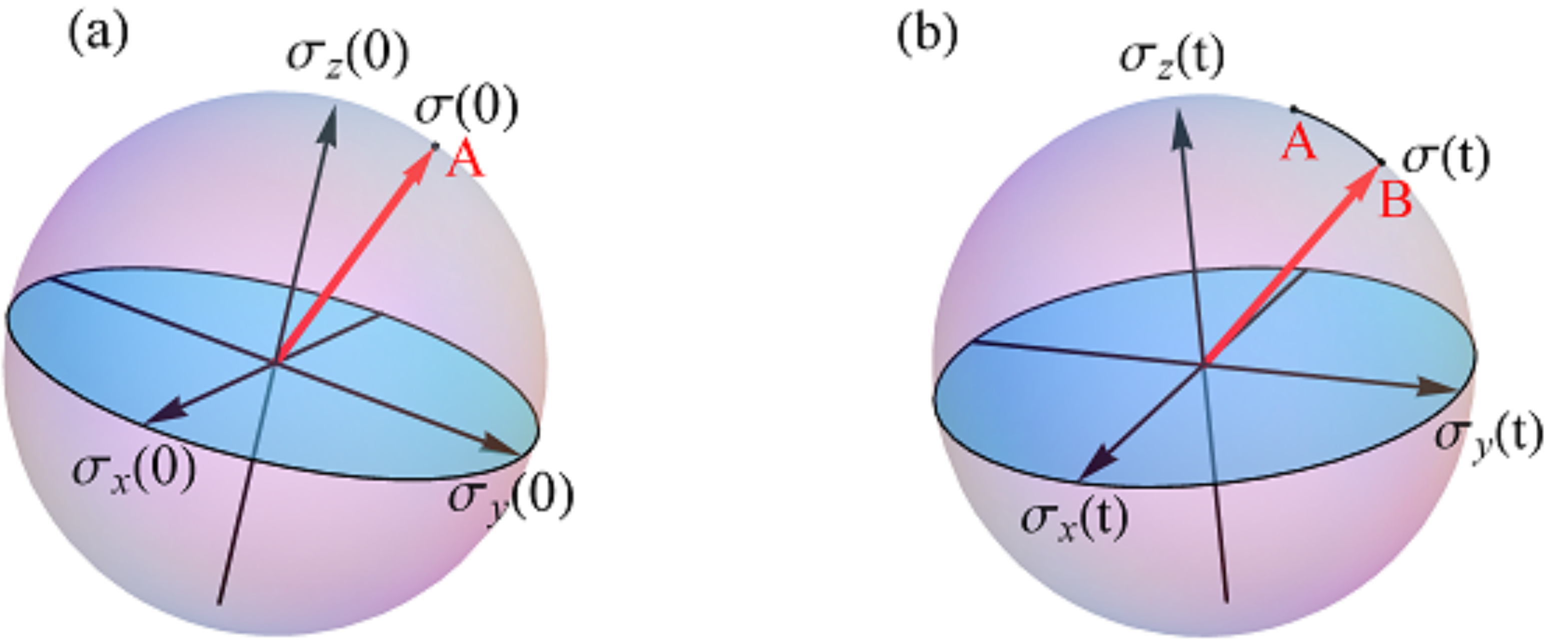

$\nabla_0 \sigma = 0$ SO coupling

$\boxed{\nabla_0 \sigma \neq 0}$ SO coupling +Higgs term

FIG. 2. Sphere surface of SU(2) gauge potential A_0. (a) At initial time t = 0, basic vectors of gauge potentialσ_x (0), σ_y (0), and σ_z(0) point to certain directions. The direction vector (red arrow) σ(0) points to A. (b) After time t, basic vectors change toσ_x (t), σ_y (t), and σ_z(t) directions. The direction vectorσ(t) changes along with basic vectors and points to B. If path AB is a parallel transportation, A_0 reduces to an Abelian gauge potential.

Higgs excitations in gauge potential

Artificial gauge potential

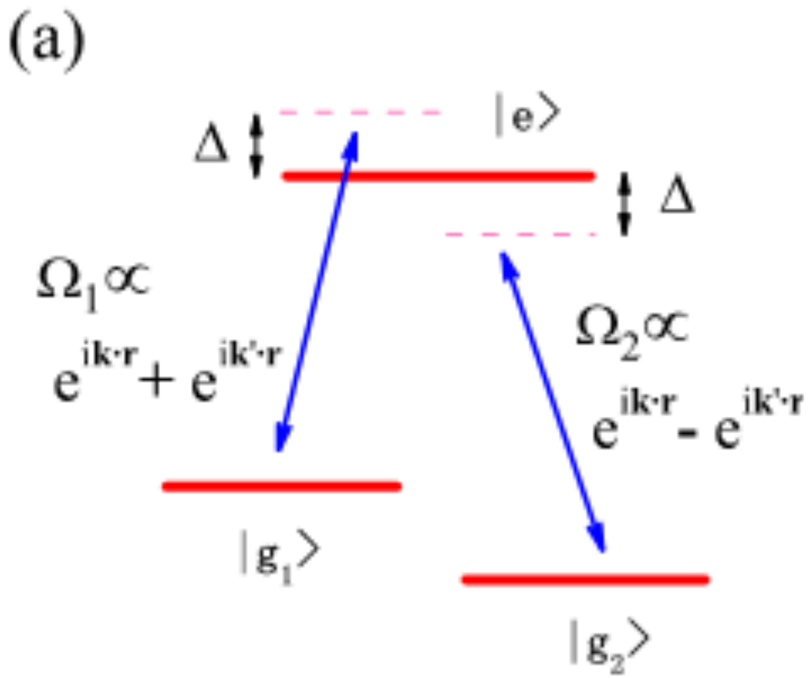

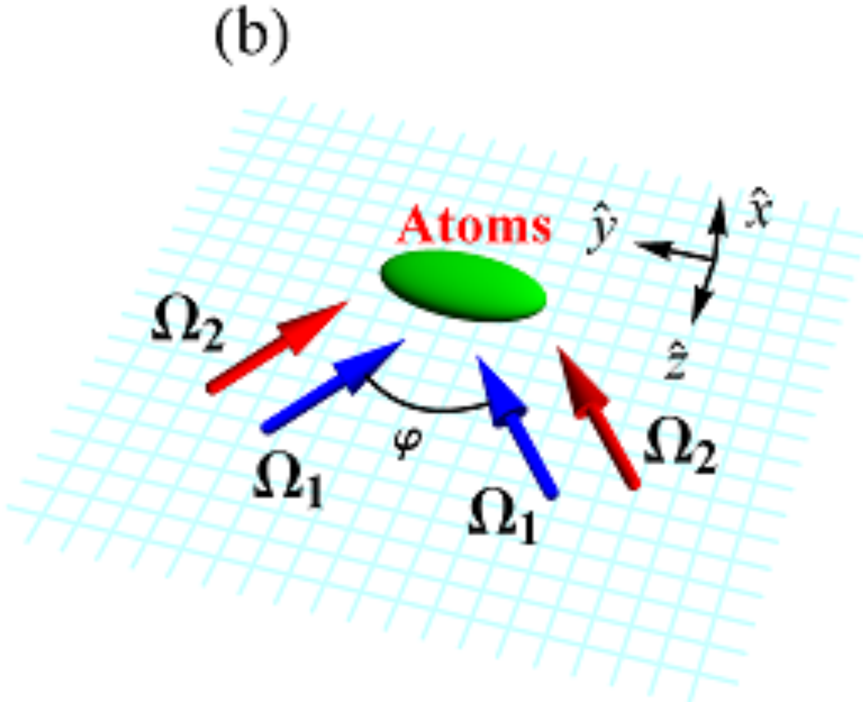

$$\boxed{A_0 = \vec{\gamma} \cdot \vec{q}\, \sigma_y + \frac{1}{2}\, \delta^2\, \overrightarrow{Q} \cdot \vec{\gamma}\, \sigma_z}$$

$$\vec{\gamma} = \vec{p}\,/\,p$$

$$\vec{q} = \vec{k} - \vec{k}'$$

$$\overrightarrow{Q} = \vec{k} + \vec{k}'$$

Decomposition of gauge potential

SO coupling

Higgs term

$$A_0 = A + B$$

Hamiltonian $H = H_k + H_{SO} + H_B$

mass term

$$H_B = H_{k,B} + \eta\, \underline{M_B}\, \sigma_z$$

$$H_{k,B} = g\, B$$

$$\mathrm{Tr}\, F_{00}\, F_{00} = M_B^2\, \mathrm{Tr}\, B \cdot B$$

(b)

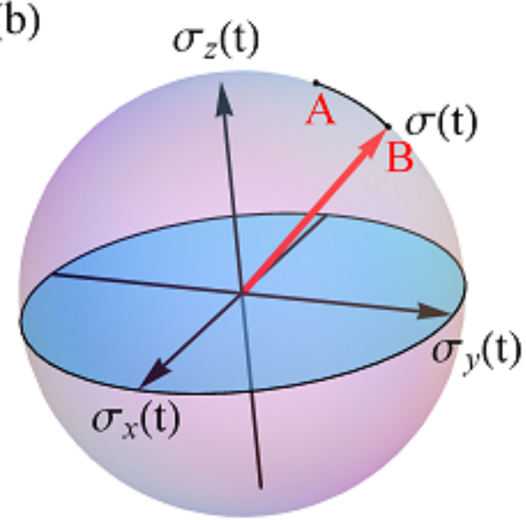

The relation between excited mass and spin Hall currents

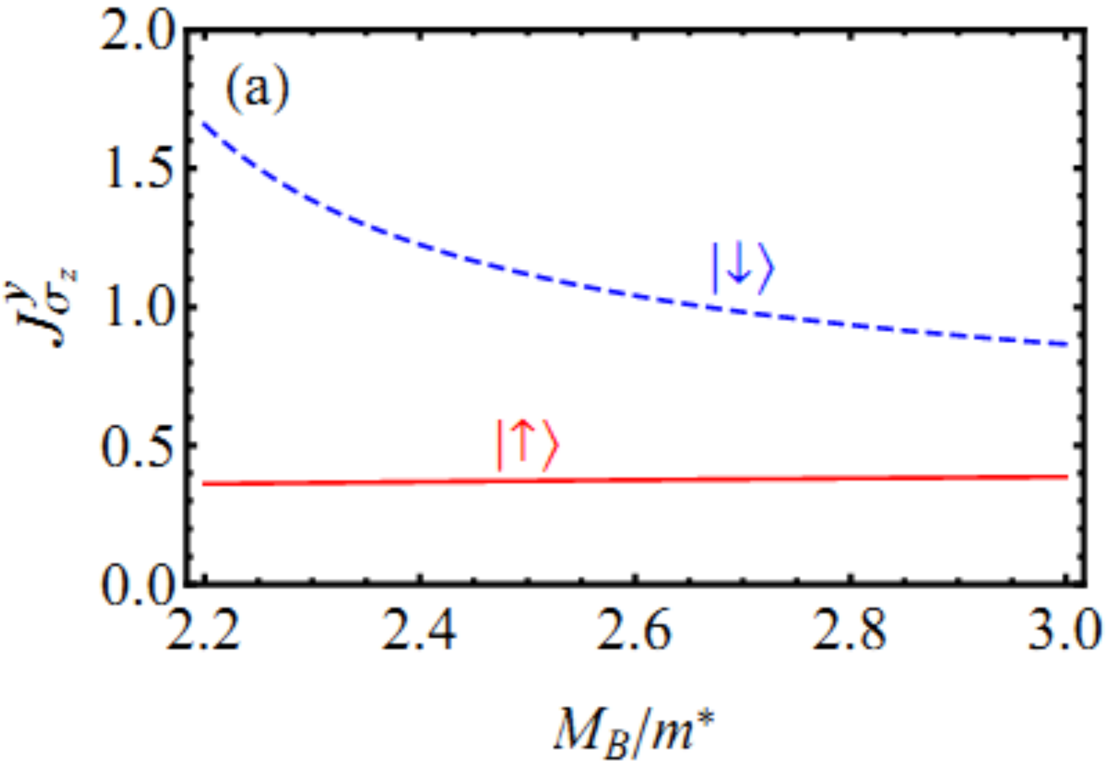

The spin down current is suppressed by the increase of the excited mass, while the spin up current grows slightly.

The evolution of atomic density profile

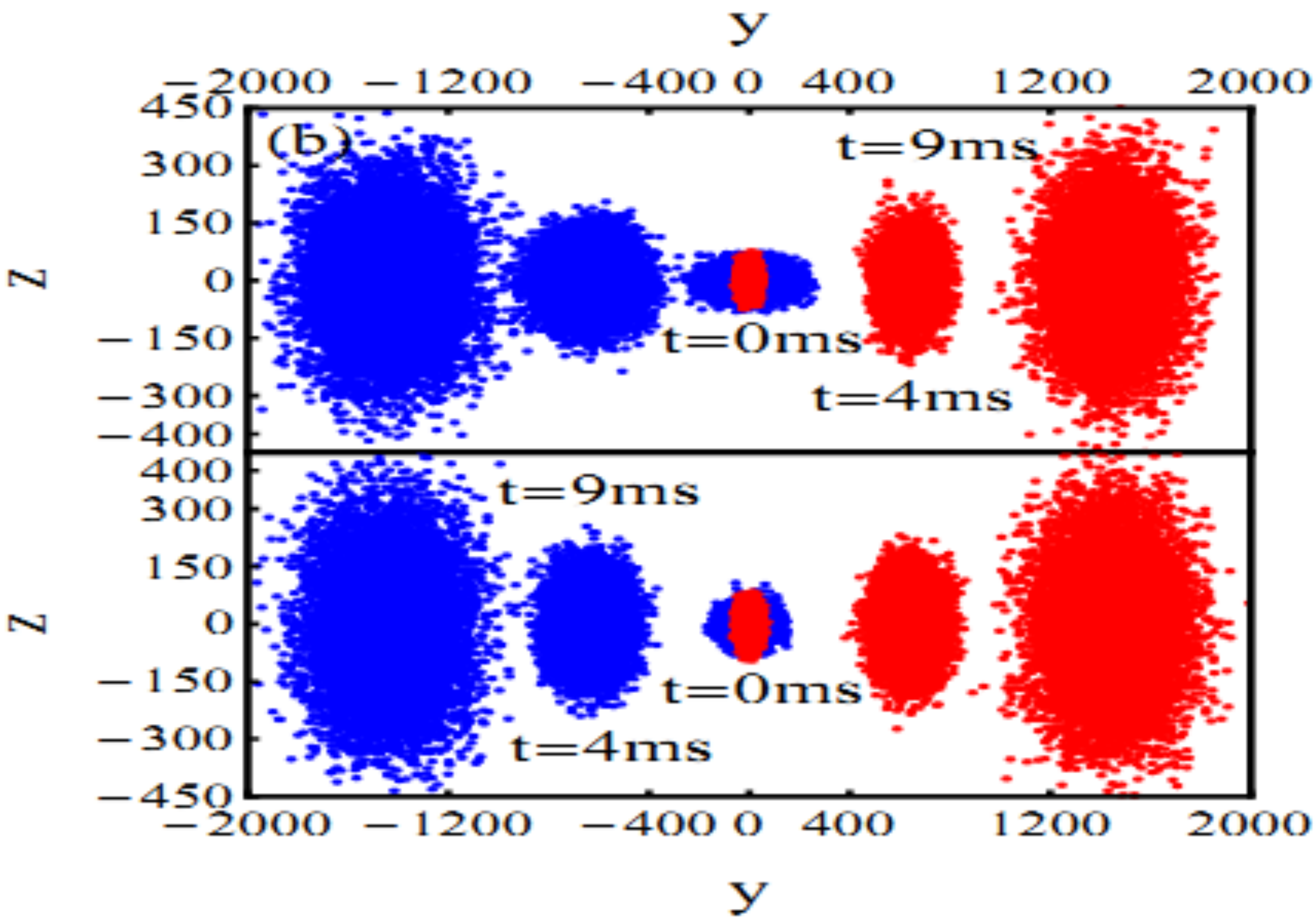

Evolution of atomic density profile from time *t*=0 ms to *t*=4ms and *t*=9ms. The spin down current is suppressed, the spin up current grows slightly. The up and down figures correspond to the ratios $M_B/m*$=2.2 and $M_B/m*$=2.8.

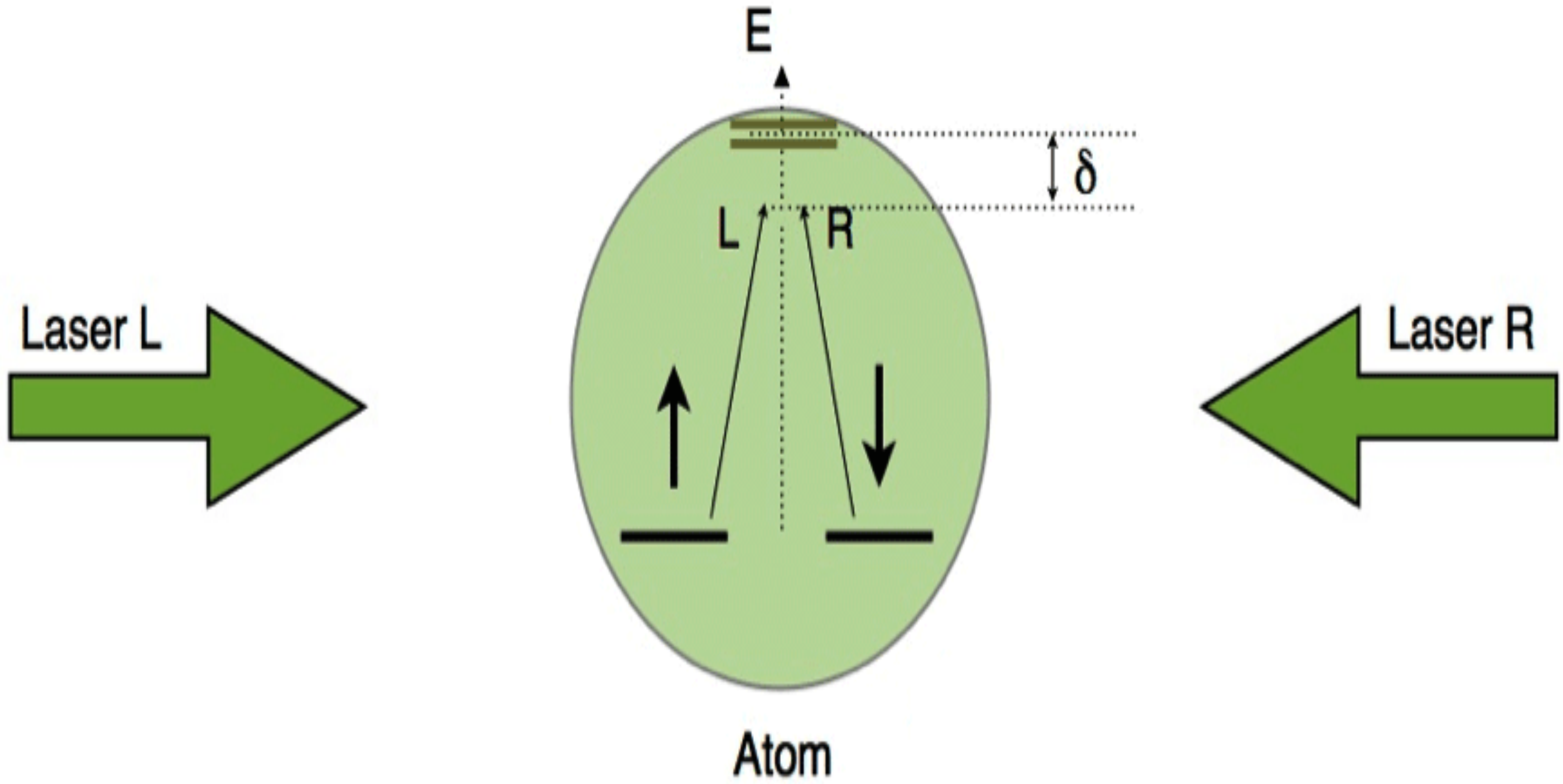

FIG. 1: Scheme for generating SOC in atomic gas. Two counter-propagating laser beams couple two spin states by a resonant two photon Raman transition: an atom in a spin-up (↑) state is excited to a virtual level by absorbing a photon from left beam, flips to spin-down (↓) state by emitting another photon into right beam. The lasers are detuned by a frequency δ from an excited multiplet.

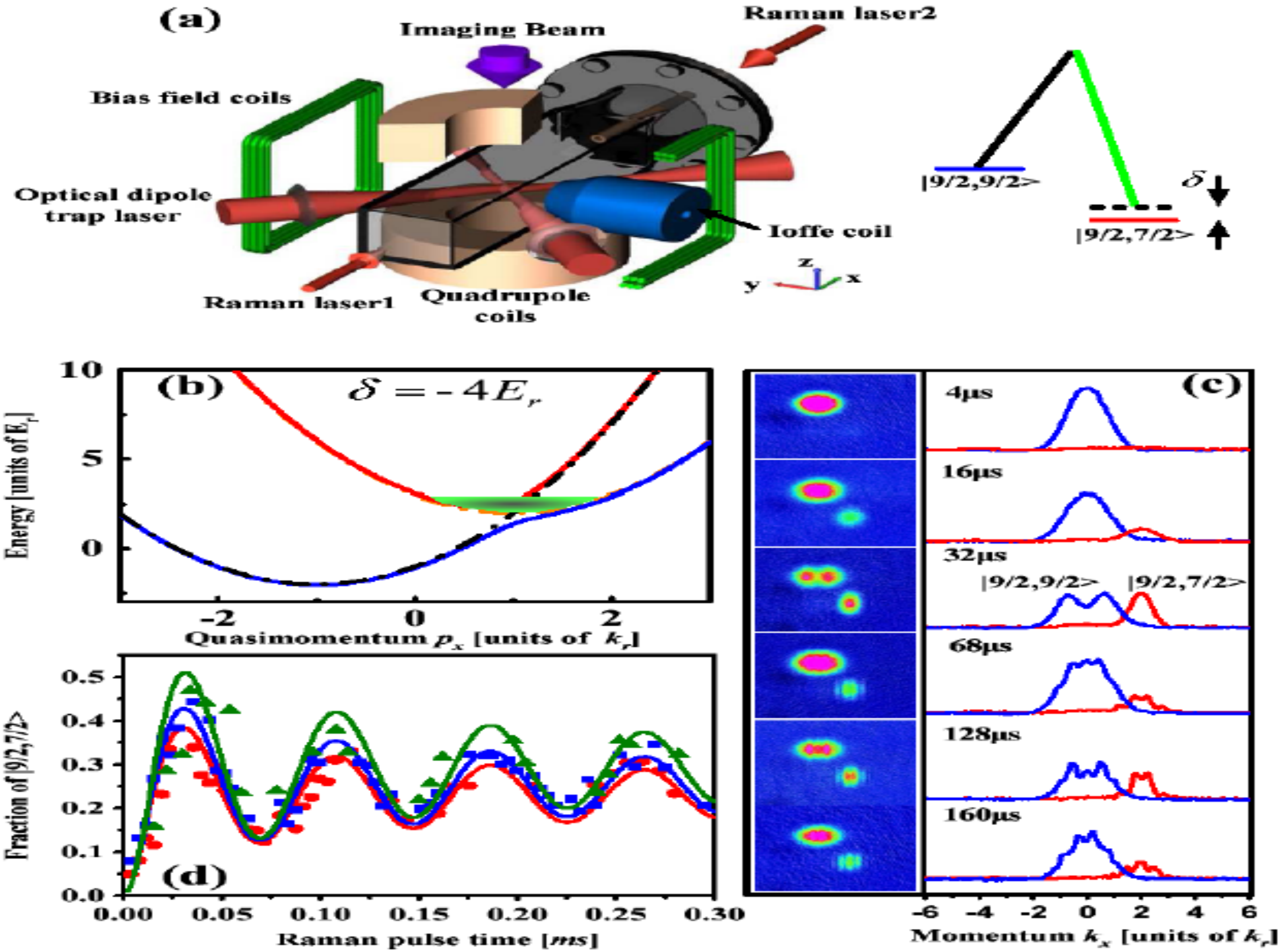

^{40}K: Jing Zhang, Phys. Rev. Lett. 109, 095301 (2012)

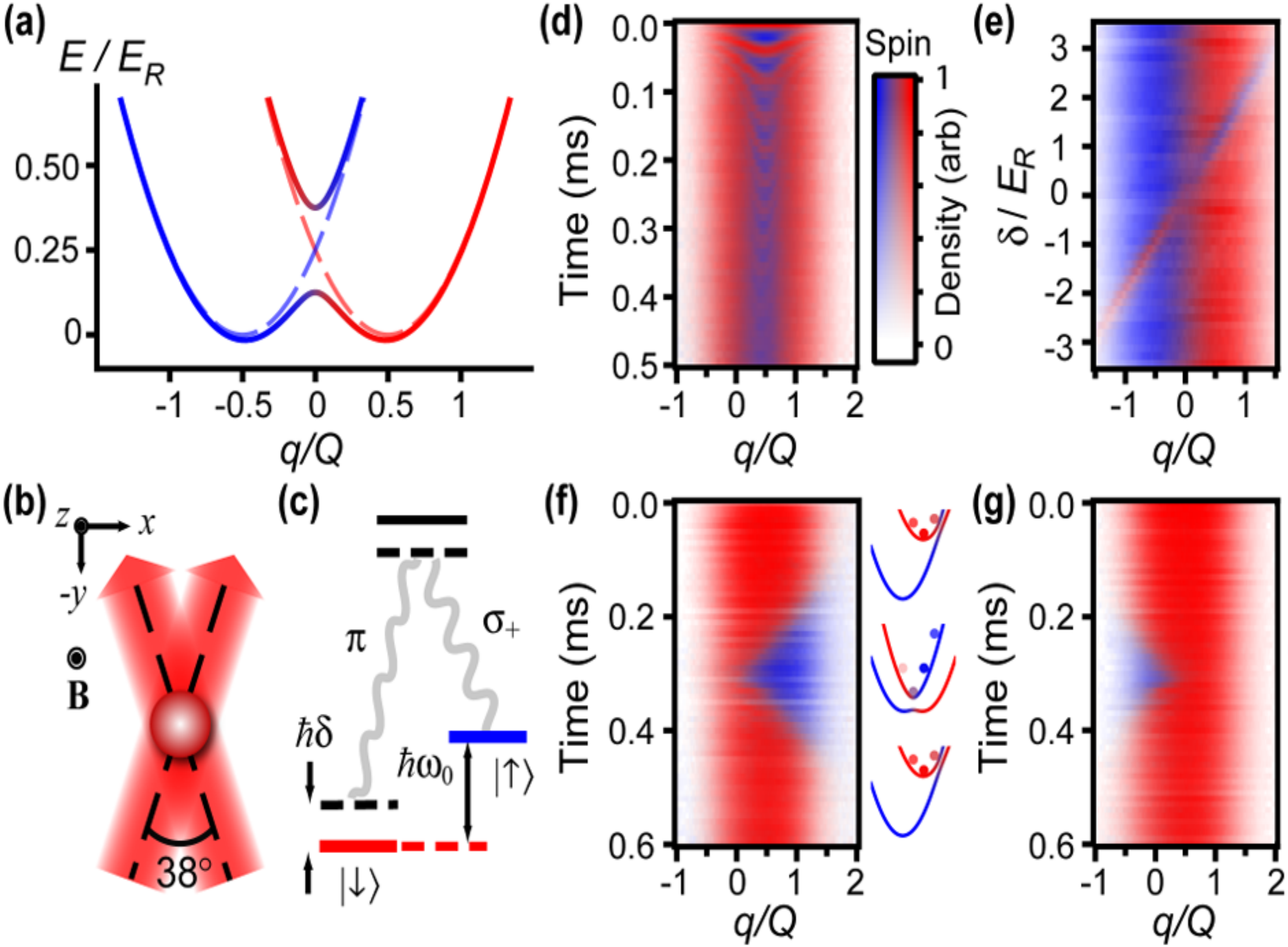

^{6}Li: M. W. Zwierlein, Phys. Rev. Lett. 109, 095302 (2012)

3. Normal state

X.L. Yu, S.S. Zhang, W.M. Liu, Phys. Rev. A 87, 043633 (2013)

$$\mathcal{H} = \mathcal{H}_0 + \mathcal{H}_I$$

$$\mathcal{H}_0 = \sum_{\mathbf{p}} c_{\mathbf{p}}^{\dagger} \left[\frac{\mathbf{p}^2}{2m} + \alpha \left(\hat{\mathbf{z}} \times \mathbf{p} \right) \cdot \sigma - \mu \right] c_{\mathbf{p}},$$

$$\mathcal{H}_I = 2g \int \frac{d^2\mathbf{k} d^2\mathbf{p} d^2\mathbf{q}}{(2\pi)^6} c_{\mathbf{k}+\mathbf{q},\uparrow}^{\dagger} c_{\mathbf{p}-\mathbf{q},\downarrow}^{\dagger} c_{\mathbf{p},\downarrow} c_{\mathbf{k},\uparrow},$$

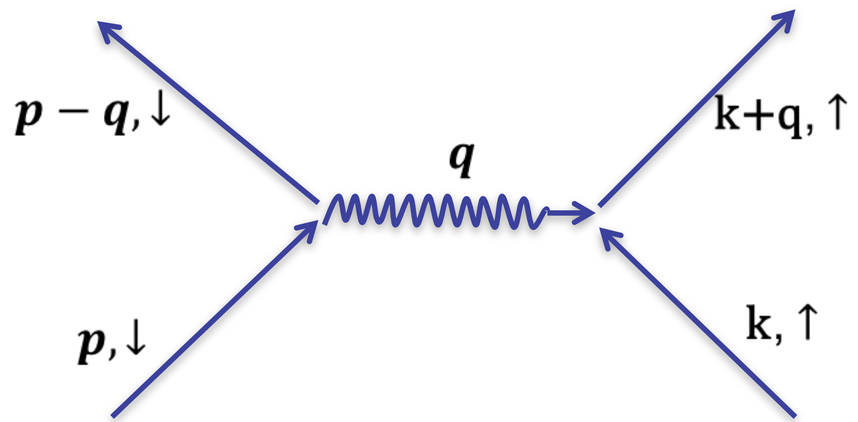

$$G_s(\mathbf{k},\omega) = \frac{1}{\omega - \xi_{\mathbf{k},s} - \Sigma_s(\mathbf{k},\omega)}$$

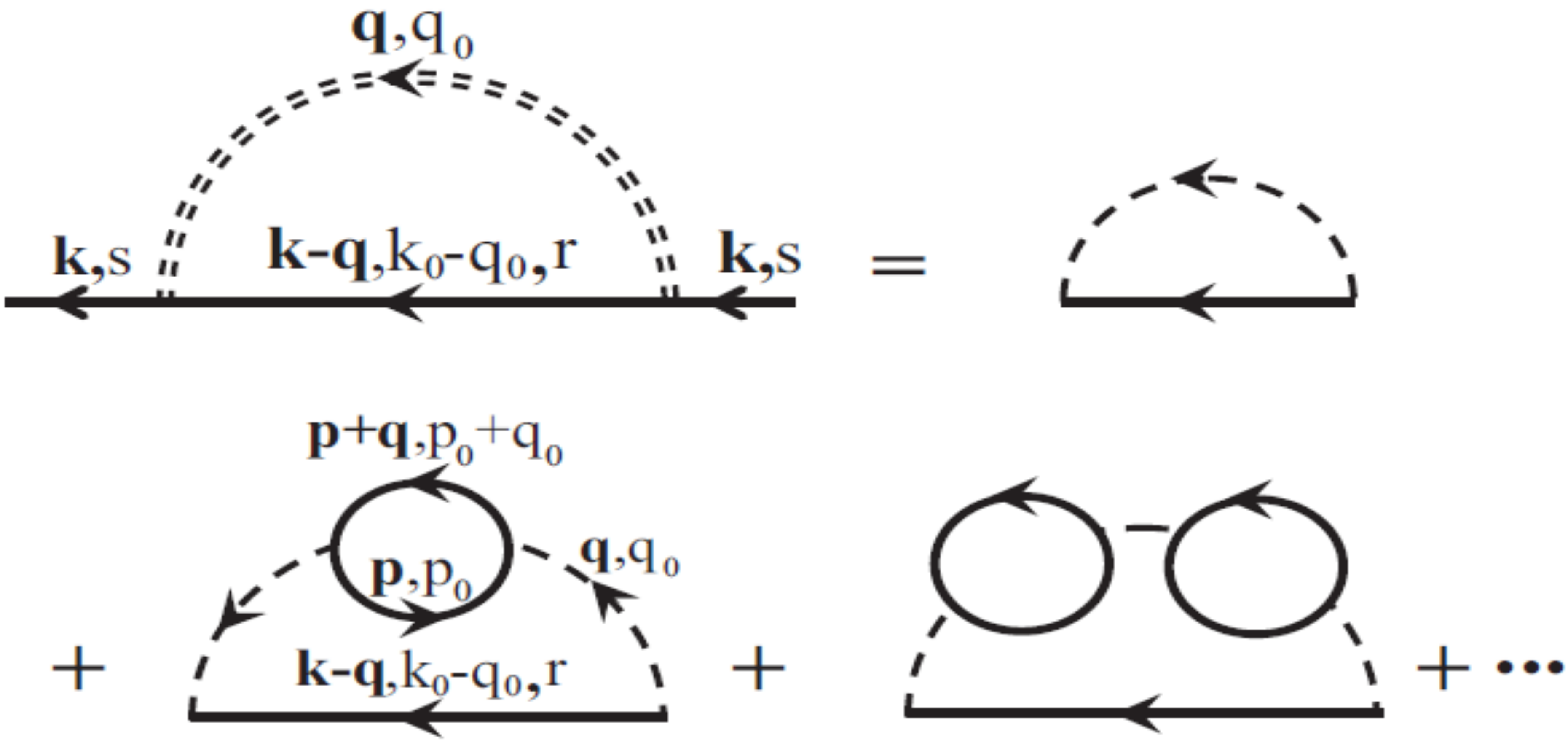

FIG. 1. Feynman diagrams for self-energy of SOC Fermi liquid in presence of *s*-wave interaction. The Feynman rules are defined under the helicity bases. The labels *s* and *r* denote helicity index. The self-energy is calculated within framework of random phase approximation.

The quasi-particle lifetime $\tau_s = 1/\Gamma_s$

$$\Gamma_s(\mathbf{k}) = -2\mathrm{Im}\Sigma_s(\mathbf{k},\xi_{\mathbf{k},s})$$

The renormalized factor

$$Z_s = \frac{1}{1-A_s}, \qquad A_s = \partial_\omega \mathrm{Re}\Sigma_s(\mathbf{k}_s,\omega)|_0.$$

The effective mass

$$\frac{m_s^*}{m} = \frac{1}{Z_s}\left(1 + \frac{m}{\kappa k_F}\partial_k \mathrm{Re}\Sigma_s^R(\mathbf{k}_s,0)\right)^{-1}$$

The spectral function

$$A(\mathbf{k},\omega) = -\frac{1}{\pi}\mathrm{Im}G^{\mathrm{ret}}(\mathbf{k},\omega)$$

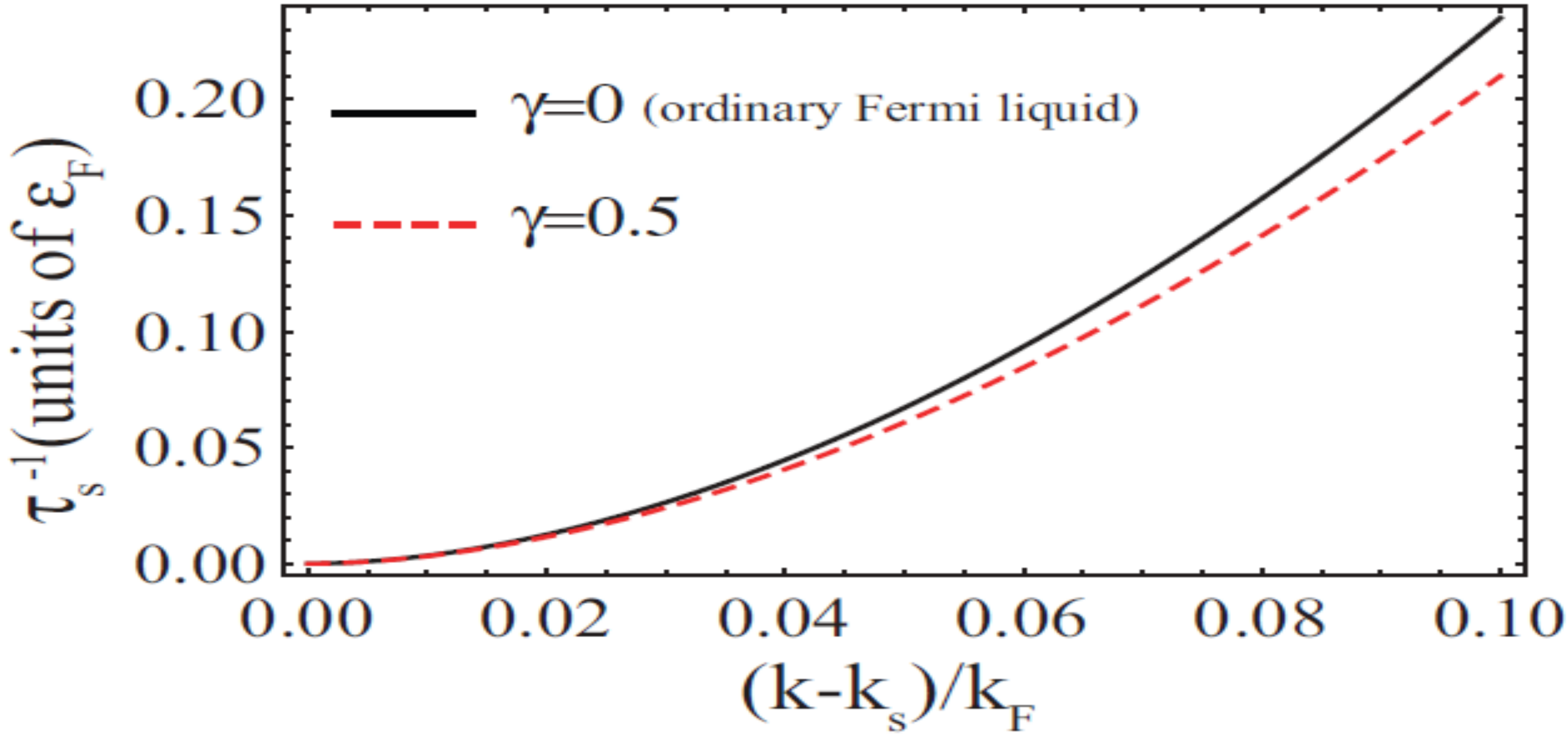

$$\Gamma_s(\mathbf{k}) = -\frac{m^2 g^2 \epsilon_F}{\pi(mg+\pi)^2}\delta^2 \left\{ \ln\frac{\delta}{8} - \frac{1}{2} - \gamma^2 \ln\frac{\gamma}{4} \right\}$$

FIG. 2. The inverse of lifetime τ_s for ^{40}K atoms as a function of momentum *k* in vicinity of Fermi surface. The lifetime of quasi-particle is enhanced due to presence of SOC.

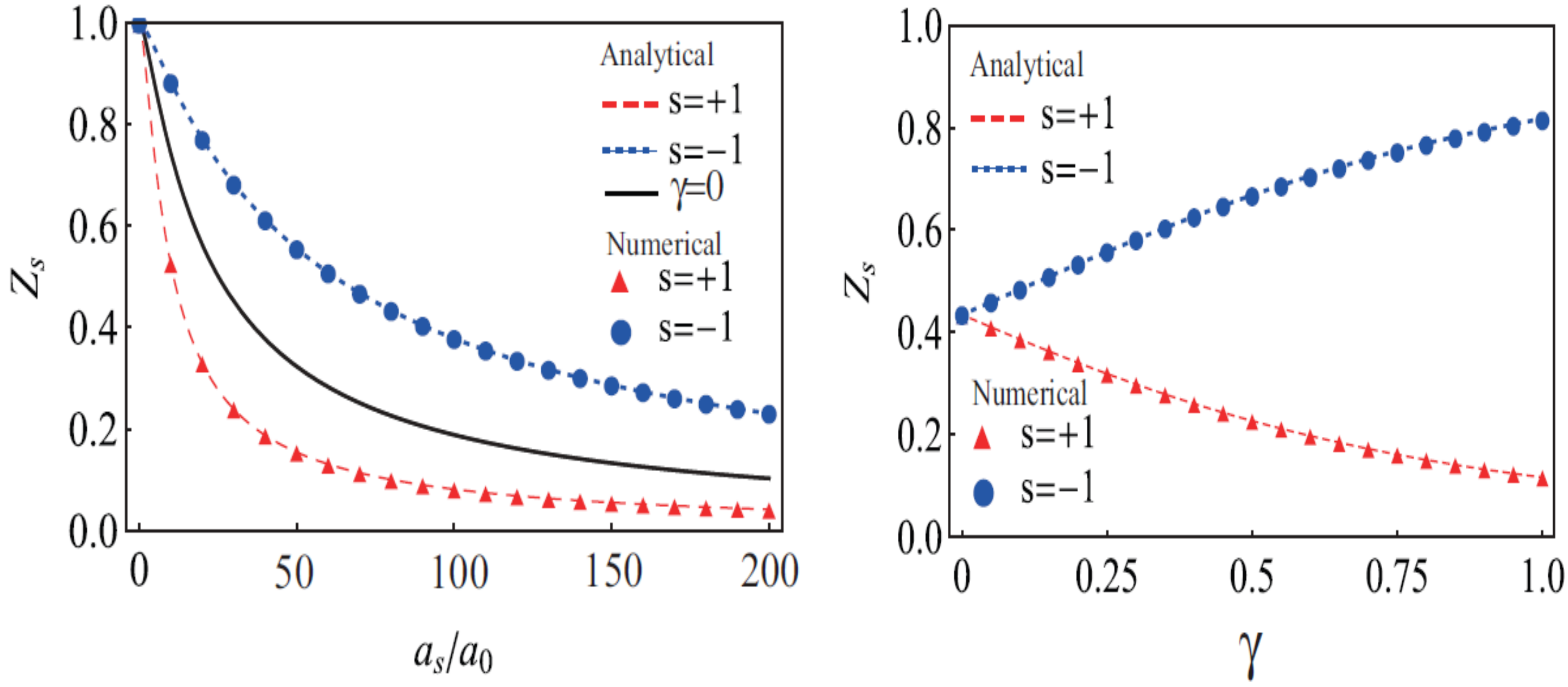

$$
\begin{aligned}
Z_s^{-1} &= 1 + \frac{m^2 g^2}{8\pi\,(mg+\pi)}\frac{1}{(\kappa - s\gamma)^2} \\
&= 1 + \frac{m^2 g^2}{8\pi\,(mg+\pi)}[1 + s\gamma + O(\gamma^2)].
\end{aligned}
$$

FIG. 3. Renormalization factor Z_s as a function of scattering length a_s *and* SOC strengthγ with same parameters as in Fig. 2.

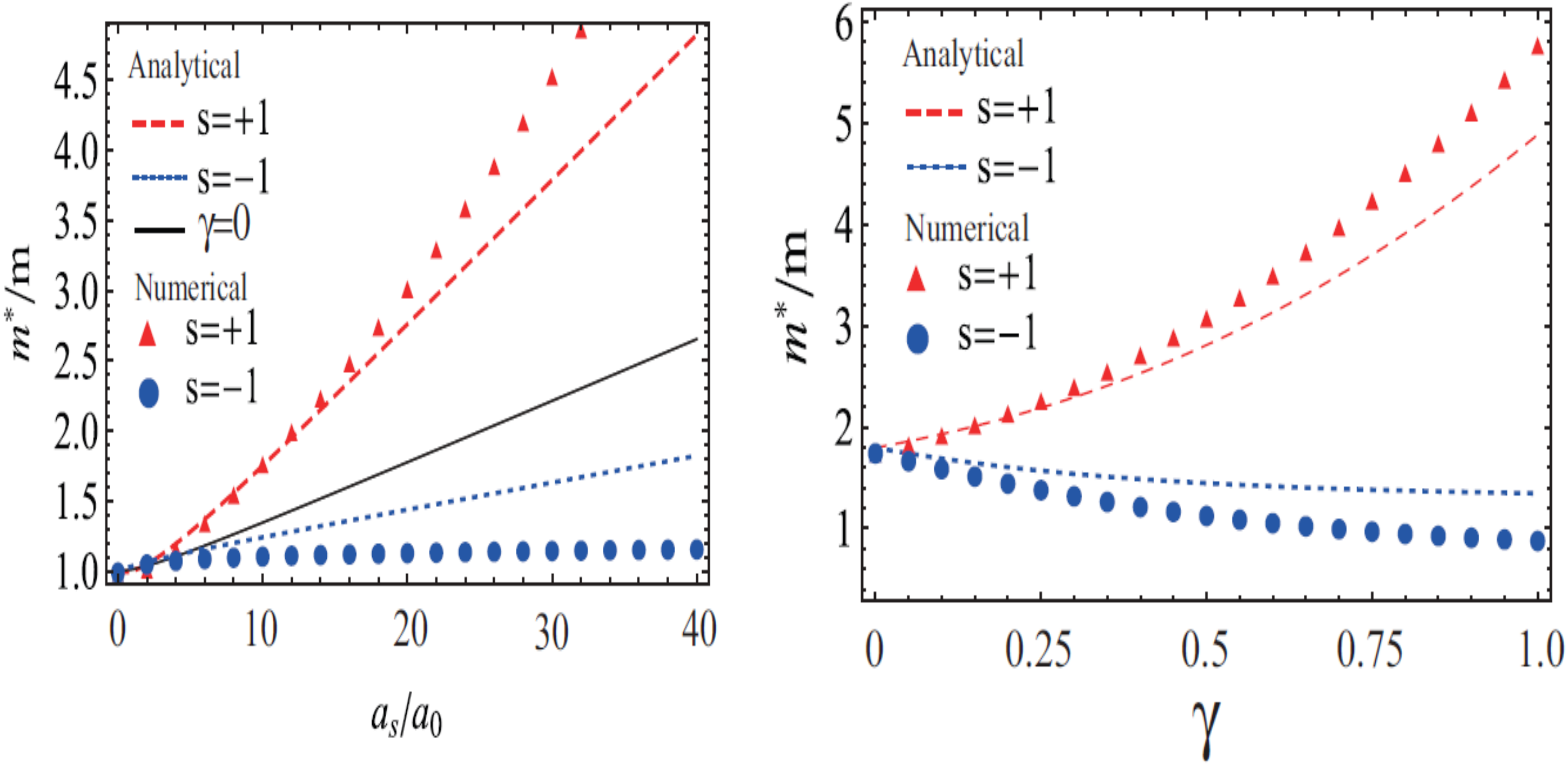

$$\frac{m_s^*}{m} = Z_s^{-1}\left(1 + s\frac{mg}{mg+\pi}\frac{\gamma}{4\kappa}\right)^{-1}$$

FIG. 4. Effective mass m*/m as a function of scattering length a_s *and* SOC strengthγ with same parameters as in Fig. 2.

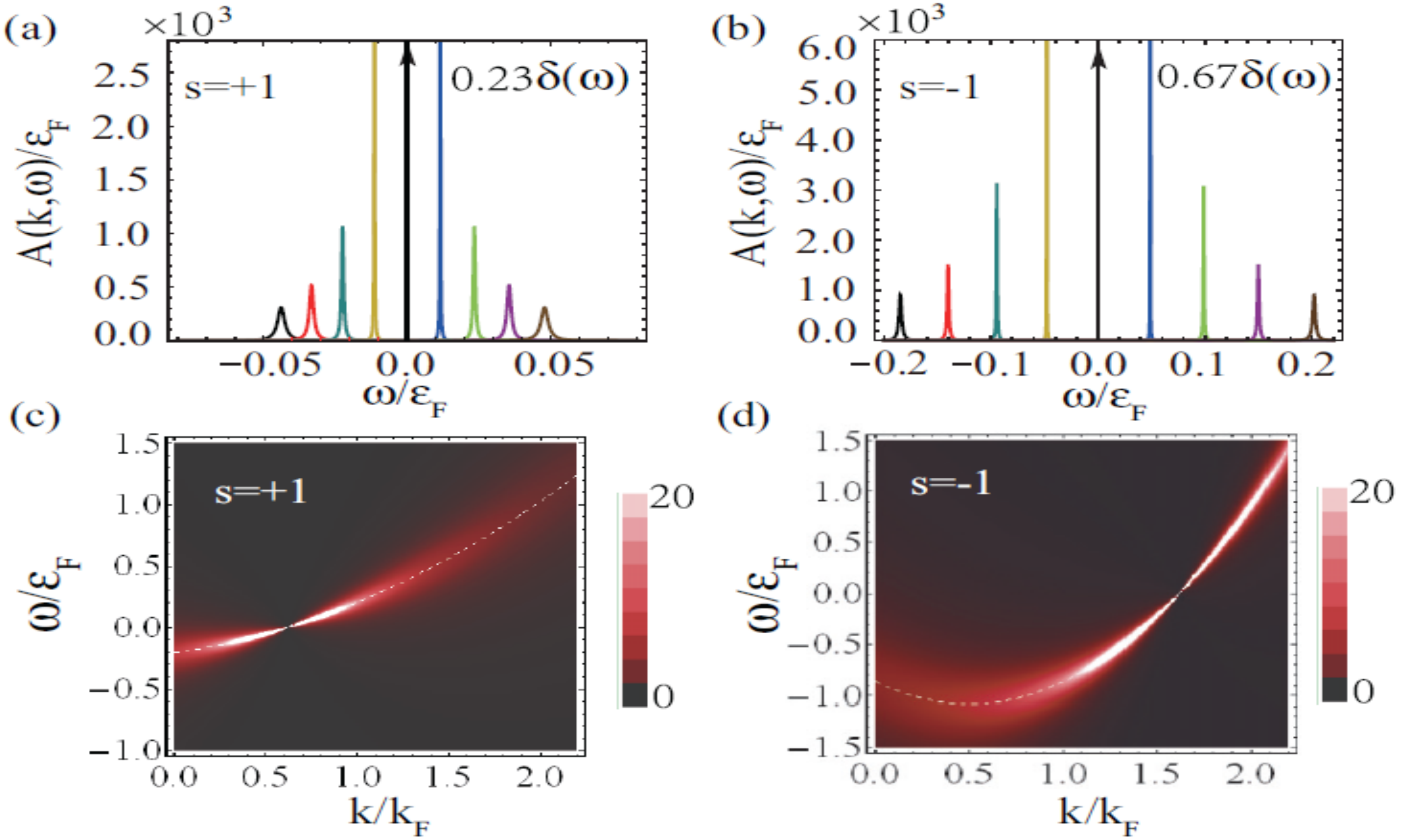

FIG. 5. Zero temperature spectral function A(k,ω) at different values of $(k - k_s)/k_F$ are shown in panels (a) and (b). Panels (c) and (d) are density plots of spectral functions for same parameters.

TABLE I. Normal-state properties for SOC Fermi liquid ($\gamma = 0.5$), ordinary Fermi liquid ($\gamma = 0$), and 2DEG ($\gamma = 0.051$) in semiconductor. All other parameters used here are the same as in Fig. 3.

	$\gamma = 0.5$	$\gamma = 0$	2DEG ($\gamma = 0.051$)[a]
$1/\tau_s$ [b]	0.73 kHz	0.67 kHz	55.36 GHz
Z_s	$Z_{+1} = 0.23$	0.96	0.97
	$Z_{-1} = 0.67$		
m_s^*/m	$m_{+1}^*/m = 4.88$	1.04	0.98
	$m_{-1}^*/m = 1.16$		

The parameters: the number of atoms is 10^4, $k_R=h/\lambda, \lambda=773$ nm, $\gamma= 0.5$, trap frequency $\omega_z=2\pi\times400$ Hz, $a_s=32a_0$, a_0 is Bohr radius. The unit $\omega_F=h\times0.21$ MHz, $(k - k_{\pm1})/k_F=0.01$.

4. Collective modes

S.S. Zhang, X.L. Yu, J.W. Ye, W.M. Liu, Phys. Rev. A 87, 063623 (2013)

$$\mathcal{H} = \sum_{\mathbf{k},\alpha,\beta} c^{\dagger}_{\mathbf{k},\alpha} h_{\alpha\beta} c_{\mathbf{k},\beta} + 2g \sum_{\mathbf{k},\mathbf{p},\mathbf{q}} c^{\dagger}_{\mathbf{k}+\mathbf{q},\uparrow} c^{\dagger}_{\mathbf{p}-\mathbf{q},\downarrow} c_{\mathbf{p},\downarrow} c_{\mathbf{k},\uparrow},$$

$$h = \frac{\mathbf{k}^2}{2m} + \lambda(\hat{\mathbf{z}} \times \mathbf{k}) \cdot \boldsymbol{\sigma} - \mu,$$

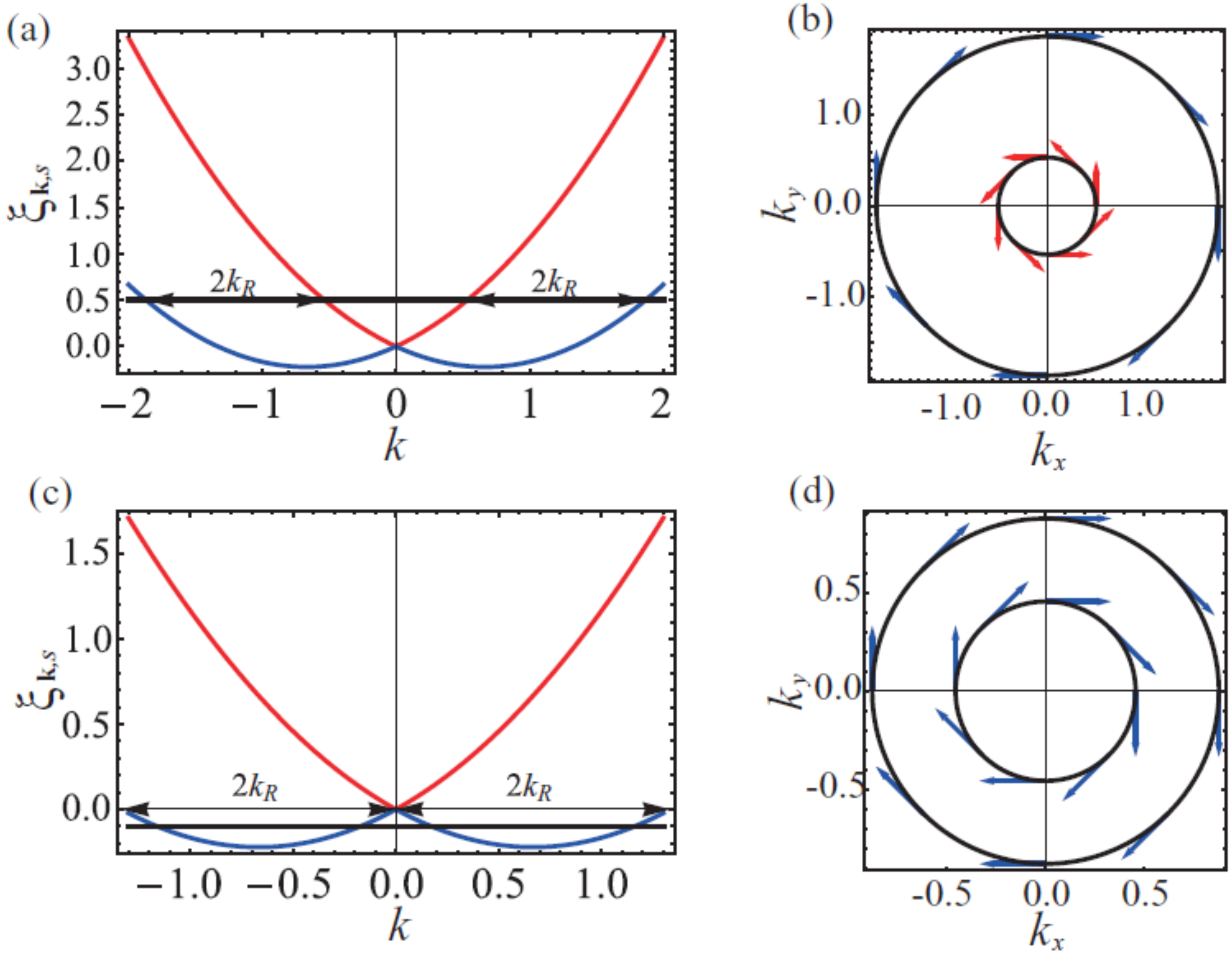

FIG. 1. (a) and (c) plot energy spectrum in presence of SOC with different fillings. The thick black horizonal line denotes level of chemical potential. (b) and (d) show Fermi surfaces and the associated spin textures corresponding to (a) and (c).

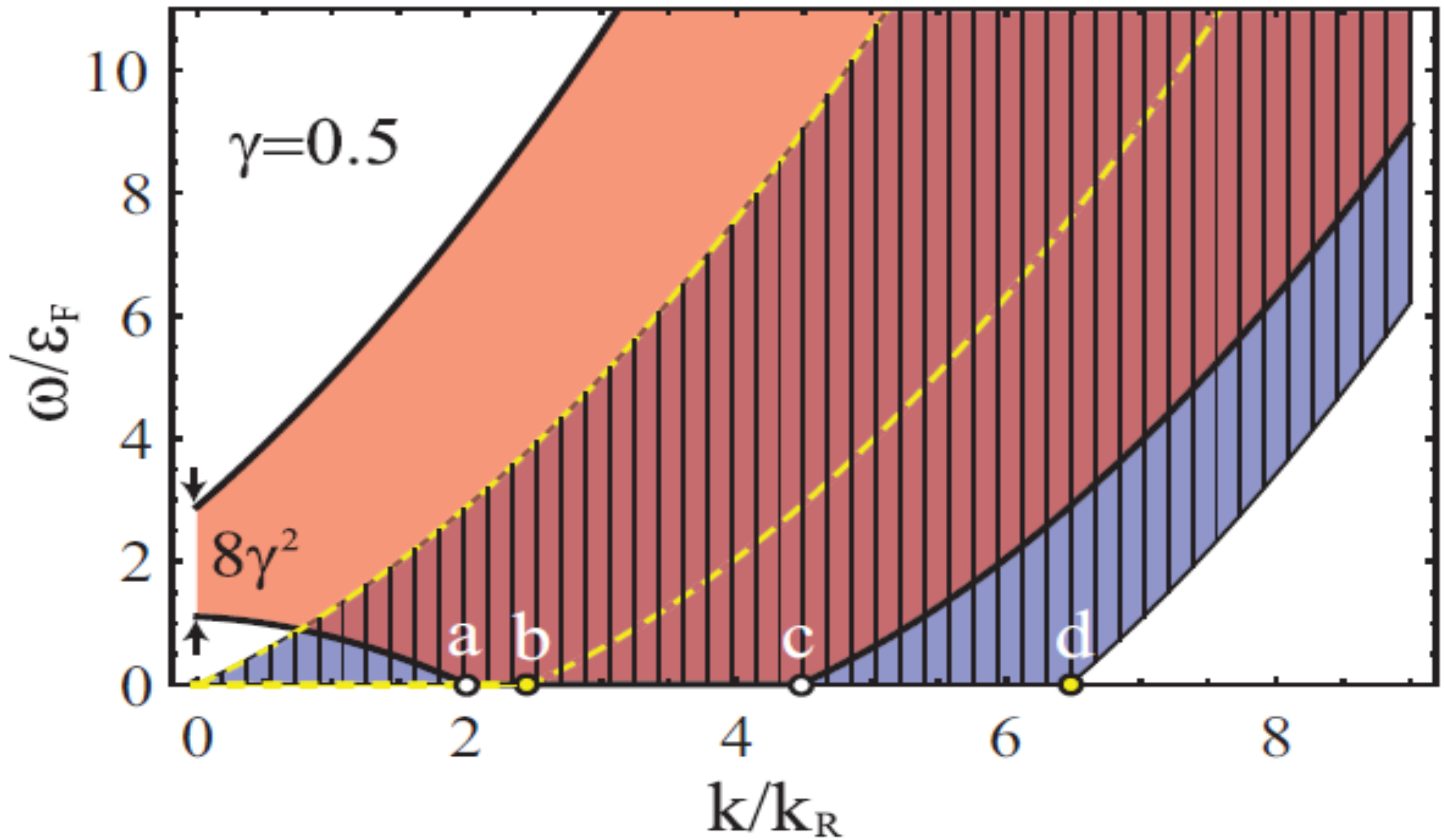

FIG. 2. Particle-hole continuum of SOC Fermi gas forγ=0.5. The red region surrounded by thick black lines represents inter-band particle-hole continuum. The region surrounded by dashed yellow lines represents continuum of intra-band particle-hole excitations with helicity +1, the blue region filled with vertical lines with helicity −1. The points *a*,*b*,*c*, *d* correspond to momenta $2k_R$, $2k_{+1}$, $2\kappa k_F$, $2k_{-1}$, where static susceptibility function exhibits singular behaviors.

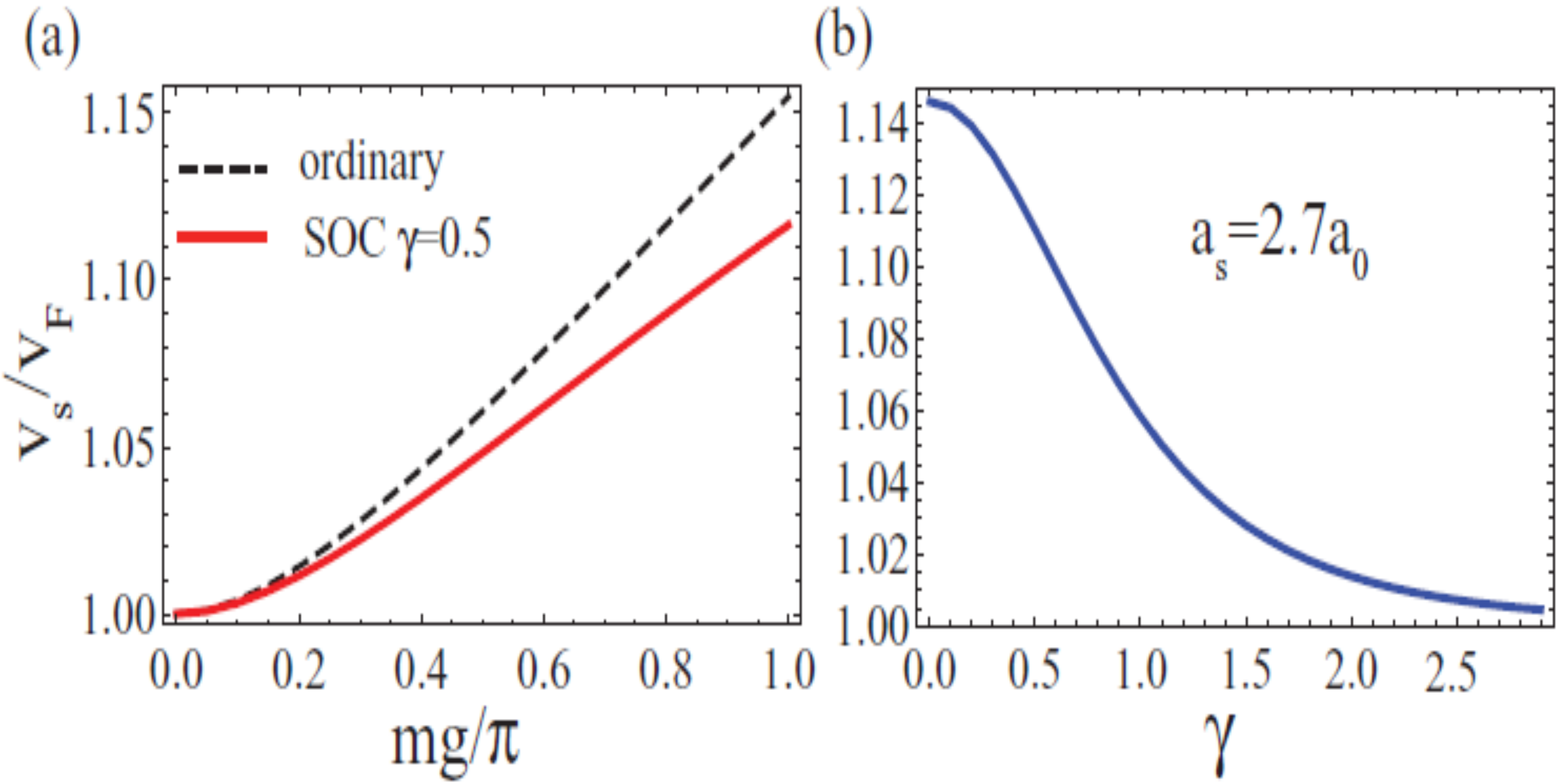

FIG. 3. The speed of zero sound as a function of *s*-wave scattering length *mg* (a) and SOC strength λ(b), the number of ^{40}K atoms is about 10^4, $k_R=2\pi/\lambda, \lambda=773$ nm, $\gamma=0.5$, trapping frequencies $(\omega_\perp, \omega_z)=2\pi \times (10{,}400)$ Hz, $a_s=2.70a_0$, a_0 is Bohr radius. The corresponding dimensionless interaction strength *mg* is about 3.0, which is less than critical valueπ.

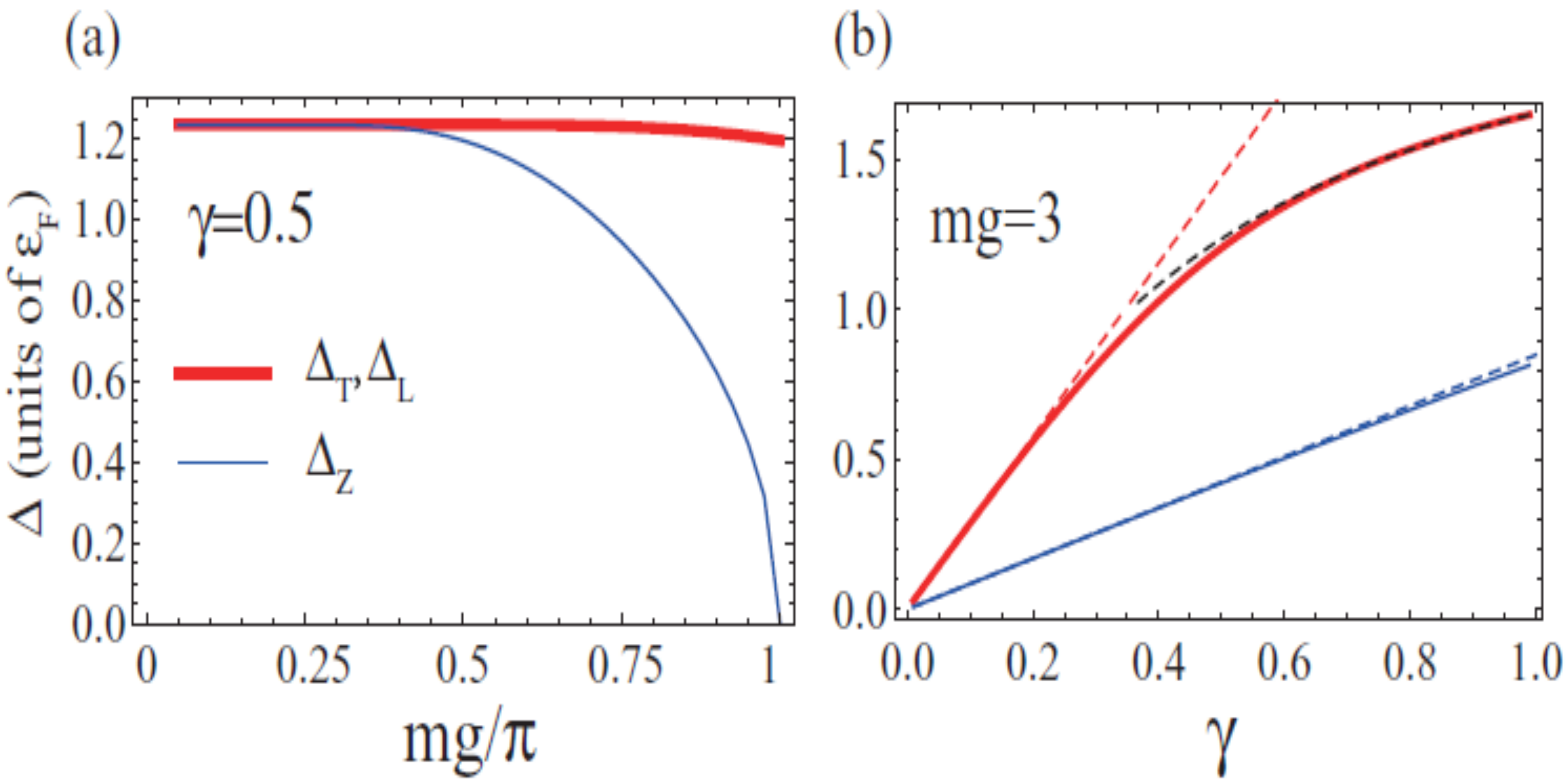

FIG. 4. The energy gaps for gapped modes as functions of dimensionless interaction strength *mg* in (a), SOC strength *γ* in (b). For (a), the energy gaps are close to edge of particle-hole continuum for *mg/π*<0.5. For (b), the red and blue dashed lines starting from*γ*=0 are approximations in Eqs. (31) and (33), the black dashed line starting from *γ*=1 are boundary of particle-hole continuum at q=0.

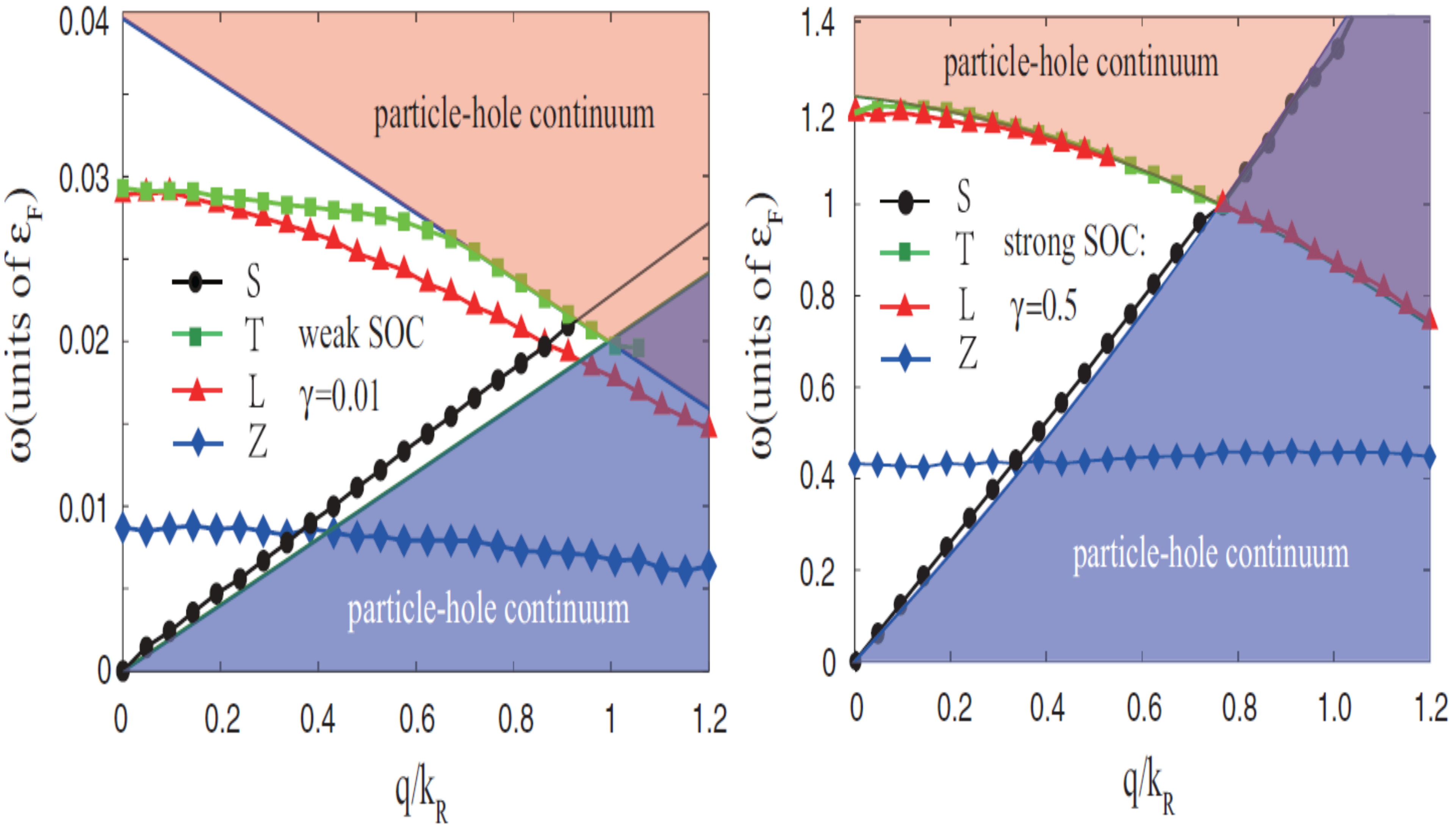

FIG. 5. The collective excitations for SOCγ=0.01 and 0.5. The transverse, longitudinal, and perpendicular spin excitations are labeled by *T, L, Z*. *S* denotes zero sound mode. These collective modes disappear in particle-hole continuum. The red region denotes spin sector of particle-hole continuum and the blue region denotes density sector.

5. Itinerant ferromagnetism

S.S. Zhang, J.W. Ye, W.M. Liu, arXiv:1403.7031

$$\mathcal{H} = \sum_{\mathbf{k},\alpha,\beta} \Psi^{\dagger}_{\mathbf{k},\alpha} \left(\frac{\hbar^2 \mathbf{k}^2}{2m} + \lambda \mathbf{k} \cdot \boldsymbol{\sigma} - \mu \right)_{\alpha,\beta} \Psi_{\mathbf{k},\beta}$$

$$+g \sum_{\mathbf{k},\mathbf{p},\mathbf{q}} \Psi^{\dagger}_{\mathbf{k}+\mathbf{q},\uparrow} \Psi^{\dagger}_{\mathbf{p}-\mathbf{q},\downarrow} \Psi_{\mathbf{p},\downarrow} \Psi_{\mathbf{k},\uparrow},$$

$$\lambda = \frac{g_F \mu_B \nabla B}{3m\hbar}$$

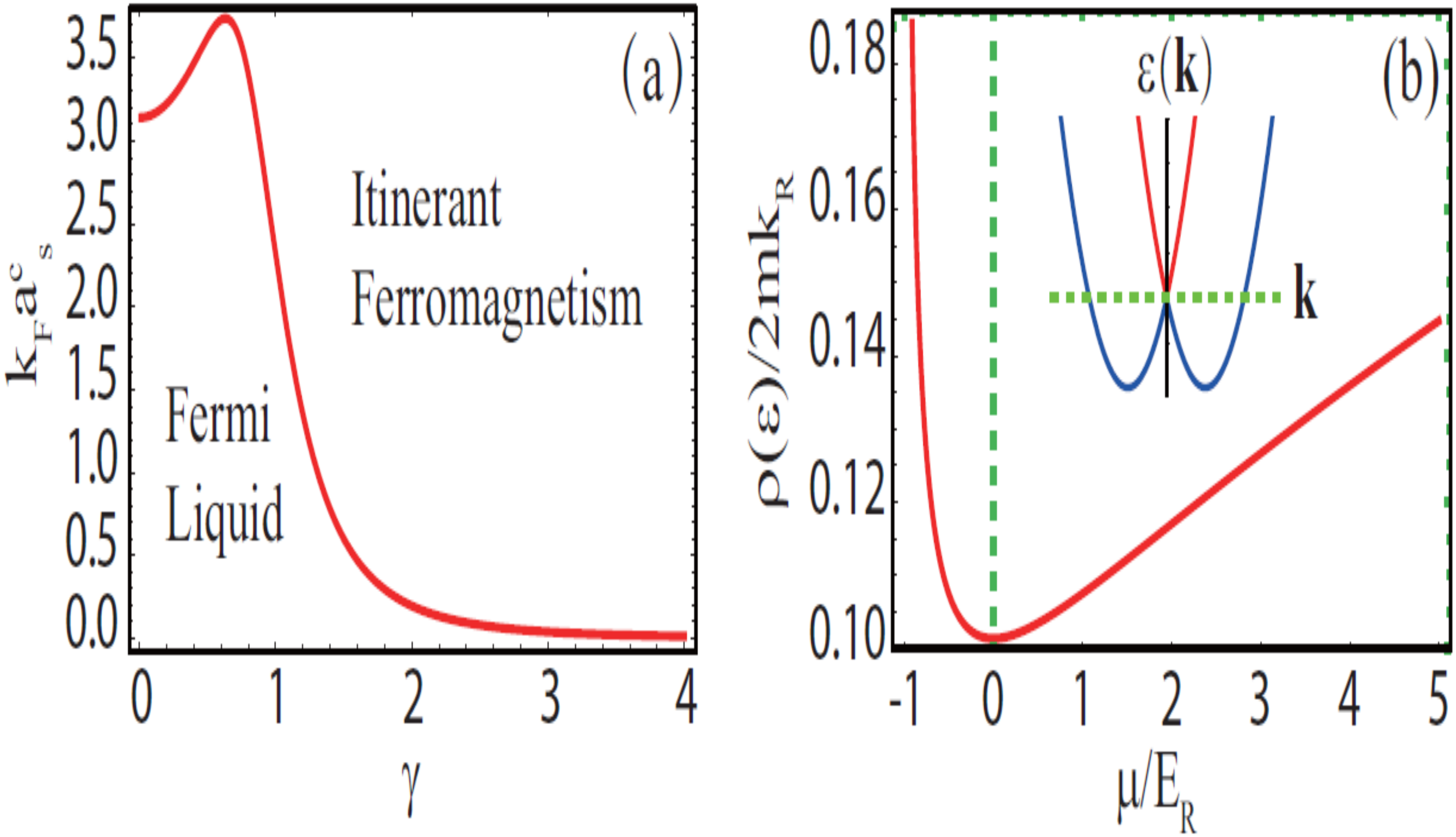

FIG. 1 (a) Critical interaction strength $k_F a^c_s$ to itinerant ferromagnetism as a function of SOC strengthγ=k_R/k_F . (b) The density of states$\rho(\epsilon)$ in units of $2mk_R$ at chemical potentialμ. The green dashed line denotesμ=0 as shown by inset.

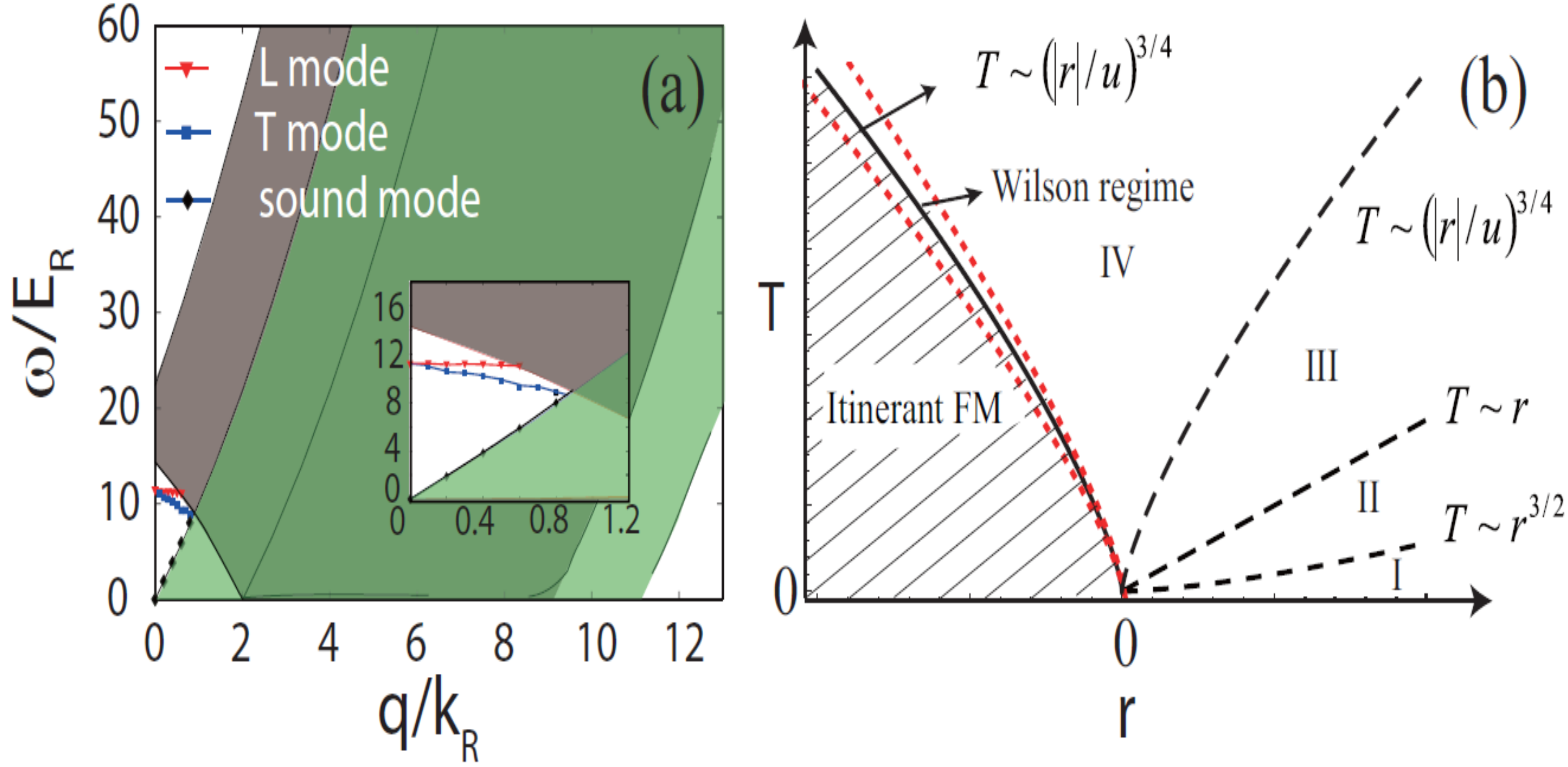

FIG. 2 (a) Collective modes and particle-hole excitation in paramagnet side at γ=0.2, $a_s=0.9a^c_s$. (b) Finite temperature quantum-classical crossovers near paramagnet to FM transition. *r* is tuning parameter of transition. The line $T \sim r^{3/2}$ ($T \sim r$) indicates quantum to classical crossover of two transverse modes (one longitudinal mode). The line between regime III and IV are given by $T \sim (|r|/u)^{3/4}$ due to irrelevant coupling *u*.

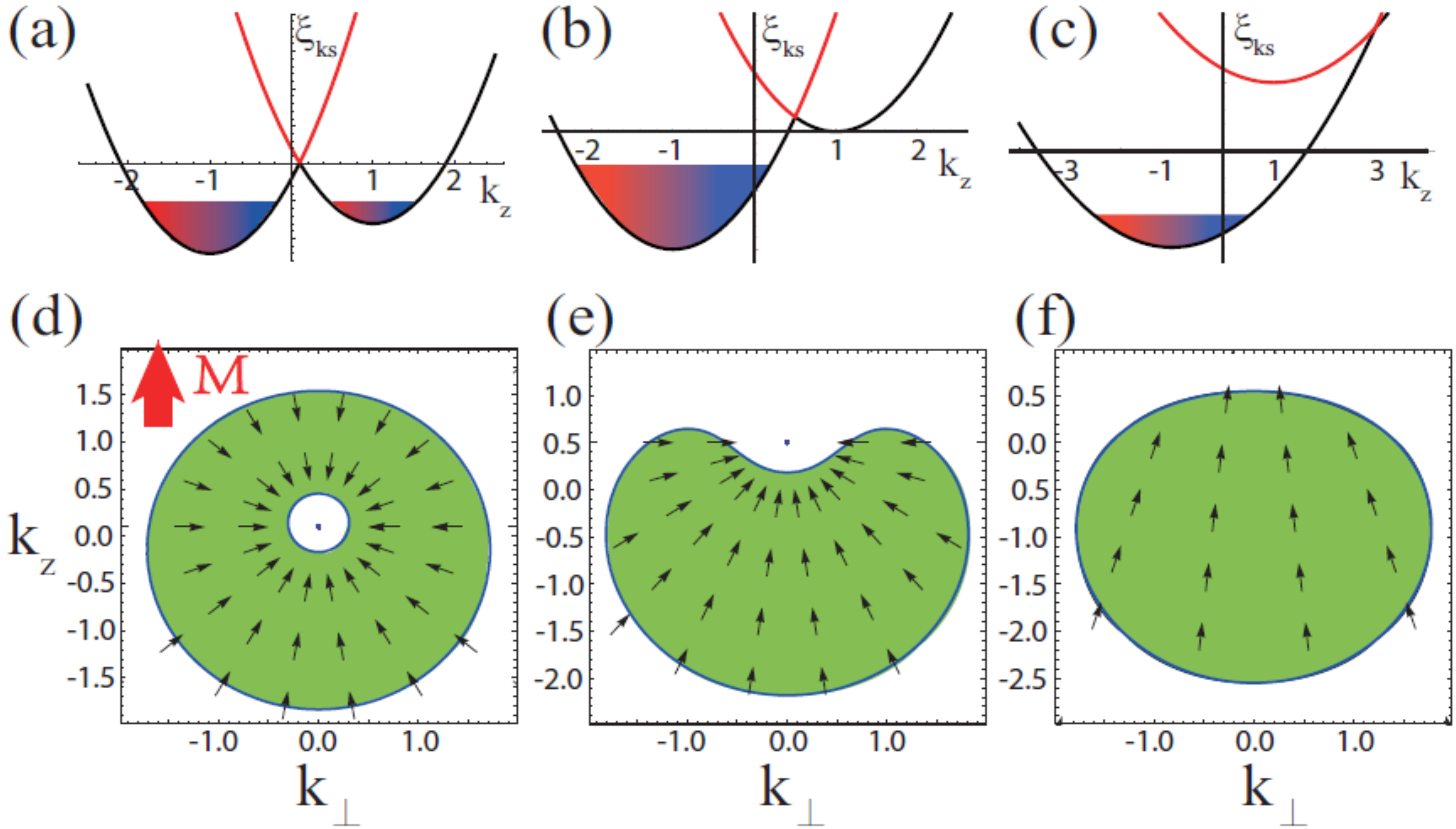

FIG. 3. The topological Lifshitz phase transition tuned by magnetizationζ, two fermi surfaces change into one nearζ~0.3. Fermionic spectrum ξ_{ks} (upper panel) and Fermi surfaces (down panel) at SOCγ=0.74 atζ=0.1 for (a),(d),ζ=0.5 for (b),(e),ζ=3 for (c),(f). The spectrum has a rotational symmetry about k_z axes. Black arrows show spin polarization.

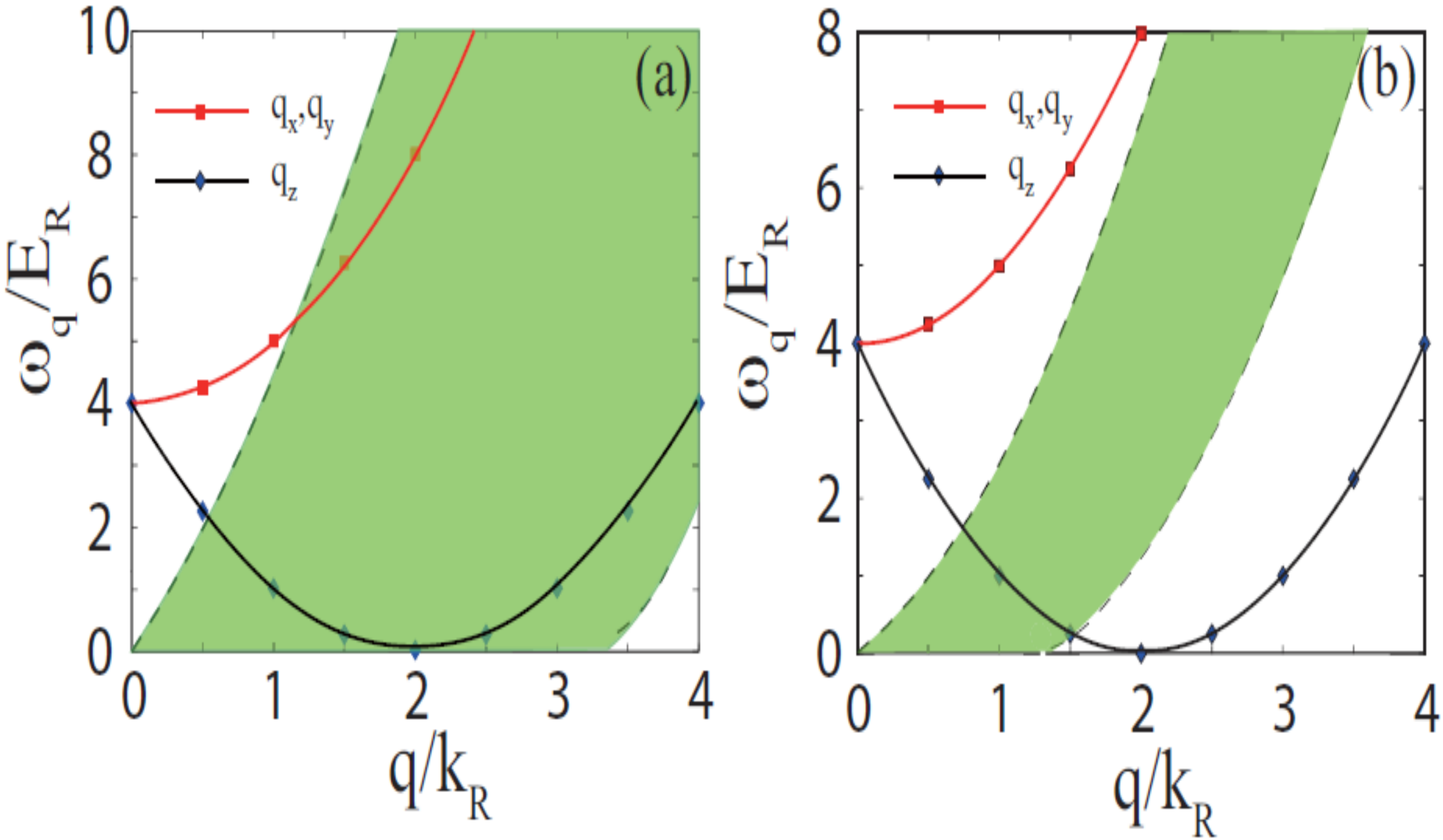

FIG. 4. The collective modes and intra-band ("−" helicity) particle-hole excitation spectrum along q_z direction (green regimes) near saturation limit$\zeta \gg 1$. (a) dense density case and (b) dilute density case. Due to its very high energy, inter-band one is outside plotrange.

5. Tricritical point

R.Y. Liao, Y.X. Yu, W.M. Liu, Phys. Rev. Lett. 108, 080406 (2012)

$$H = \int d^3\mathbf{r} \sum_{\sigma=\uparrow,\downarrow} \psi^\dagger_\sigma(\mathbf{r})\left(\frac{\hat{\mathbf{P}}^2}{2m} - \mu_\sigma\right)\psi_\sigma(\mathbf{r})$$

$$- g\int d^3\mathbf{r}\, \psi^\dagger_\uparrow(\mathbf{r})\,\psi^\dagger_\downarrow(\mathbf{r})\,\psi_\downarrow(\mathbf{r})\,\psi_\uparrow(\mathbf{r}) + H_{\mathrm{SO}}.$$

$$H_{\mathrm{SO}} = \lambda \sum_{\mathbf{k}} k_\perp [e^{-i\varphi_{\mathbf{k}}} \psi^\dagger_{\mathbf{k}\uparrow}\psi_{\mathbf{k}\downarrow} + \mathrm{H.c.}],$$

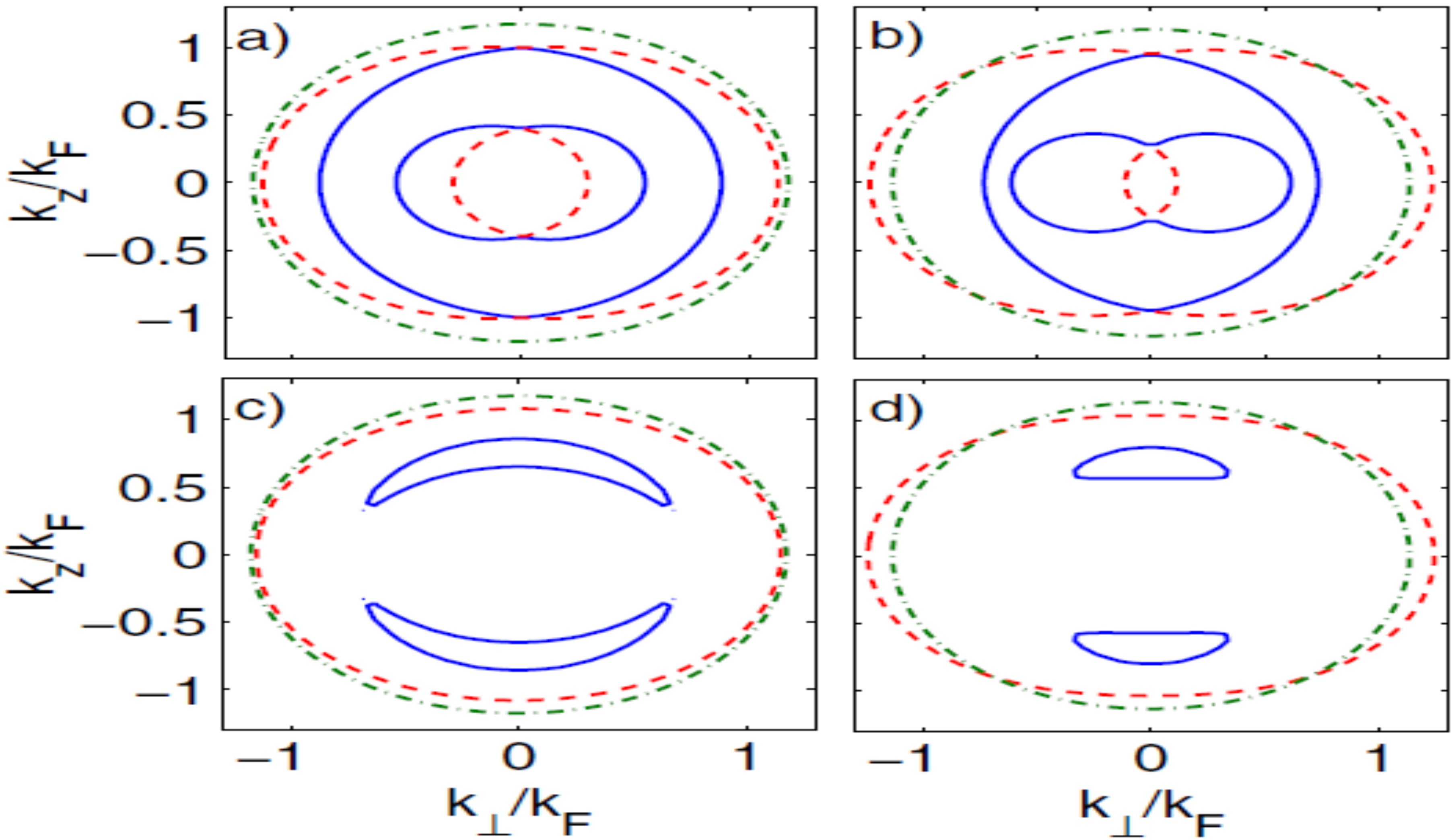

FIG. 1. Iso-energy surface ($E_{k\pm}=0.8E_F$) for quasi-particle excitation spectrum at unitarity where $1/k_Fa_s=0$ at T=0: (a) h=0,$\lambda=0.125v_F$; (b) h=0, $\lambda=0.25v_F$; (c) $h=0.1E_F$,$\lambda=0.125v_F$; (d) $h=0.1E_F$,$\lambda=0.25v_F$. The red dashed line is plotted for E_{k-}, the blue solid line is for E_{k+}, the green dash-dotted circle is for a spherical isoenergy surface.

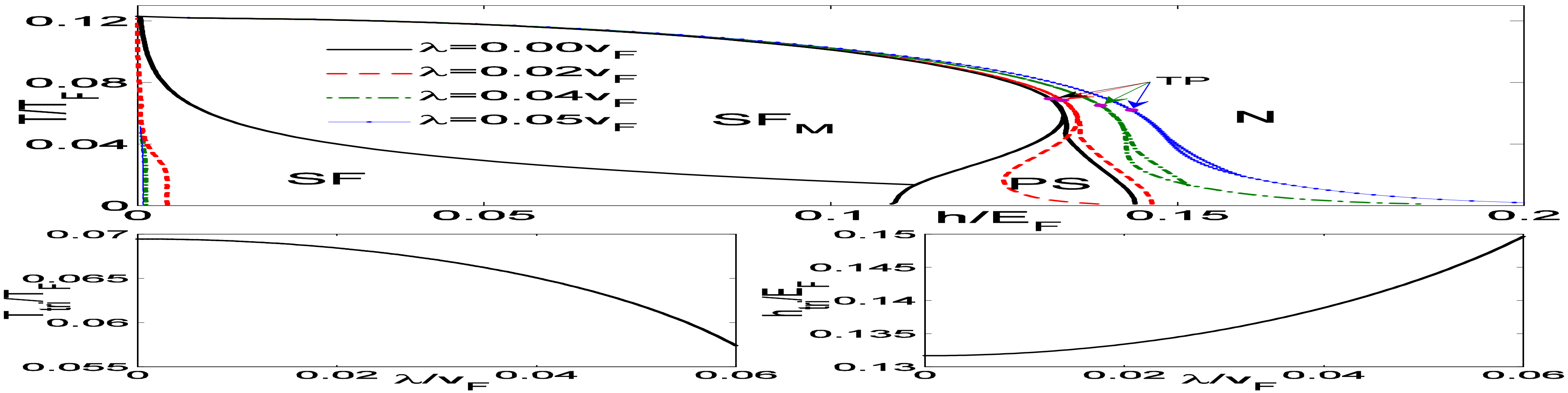

FIG. 2 Upper panel: Finite-temperature phase diagram as a function of T and h at $1/k_F a_s$=-1 (BCS side). There are four phases: N state, PS state, SF state, magnetized superfluid (SFM). Above tricritical point,transition line separating broken-symmetry state (SFM) and symmetric state (N) is of second order. Below tricritical point (TP), it changes to the first order. Lower panel: evolution of tricritical point (T_{tri}/T_F, h_{tri}/E_F) as a function of SOC strength λ.

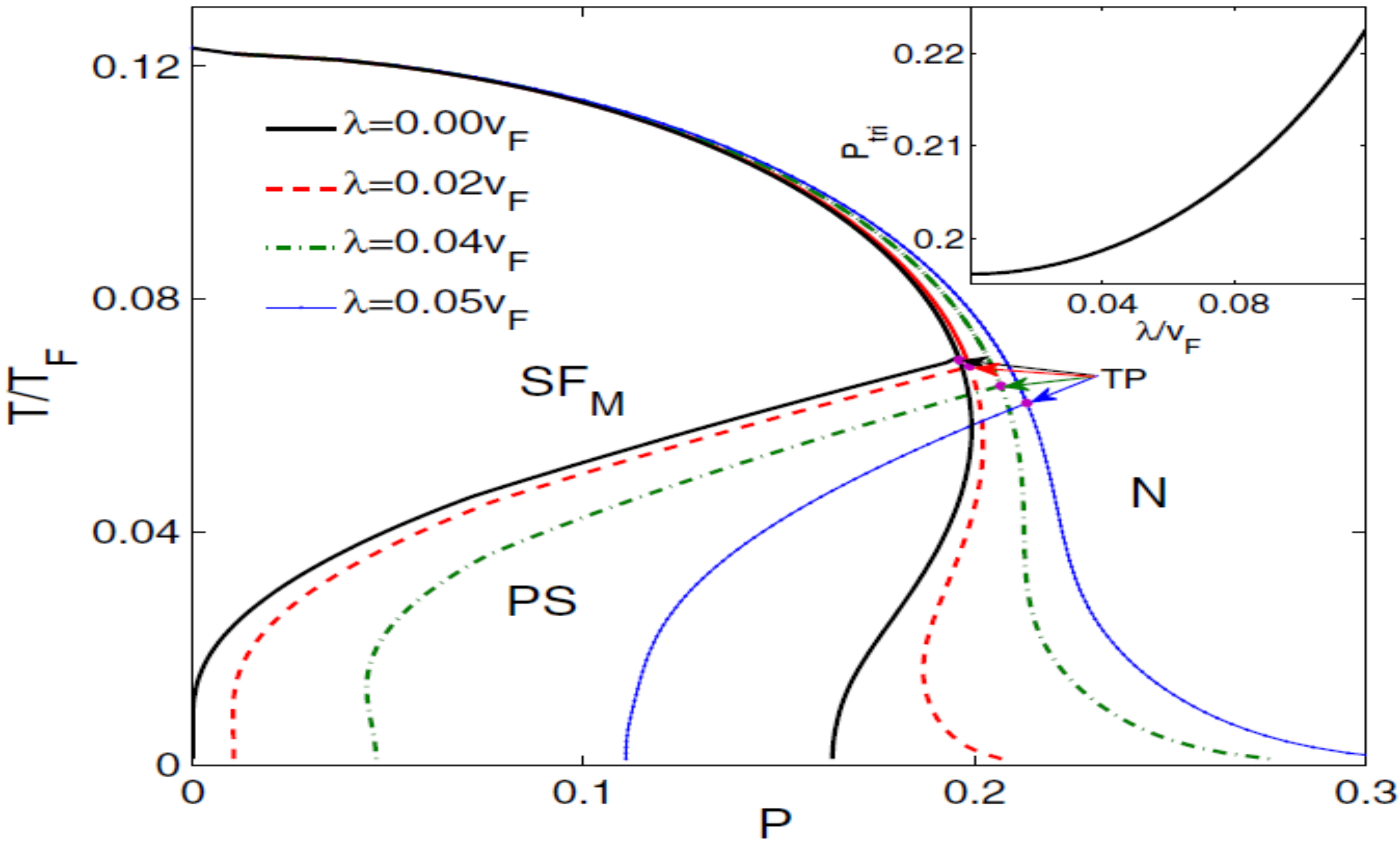

FIG. 3. Finite-temperature phase diagram in plane of T and P at $1/k_F a_s$=-1. The inset shows corresponding polarization P_{tri} for tricritical point as a function of SOC strength λ. The phase SF is along the line of P=0. The notation is the same as in Fig. 2.

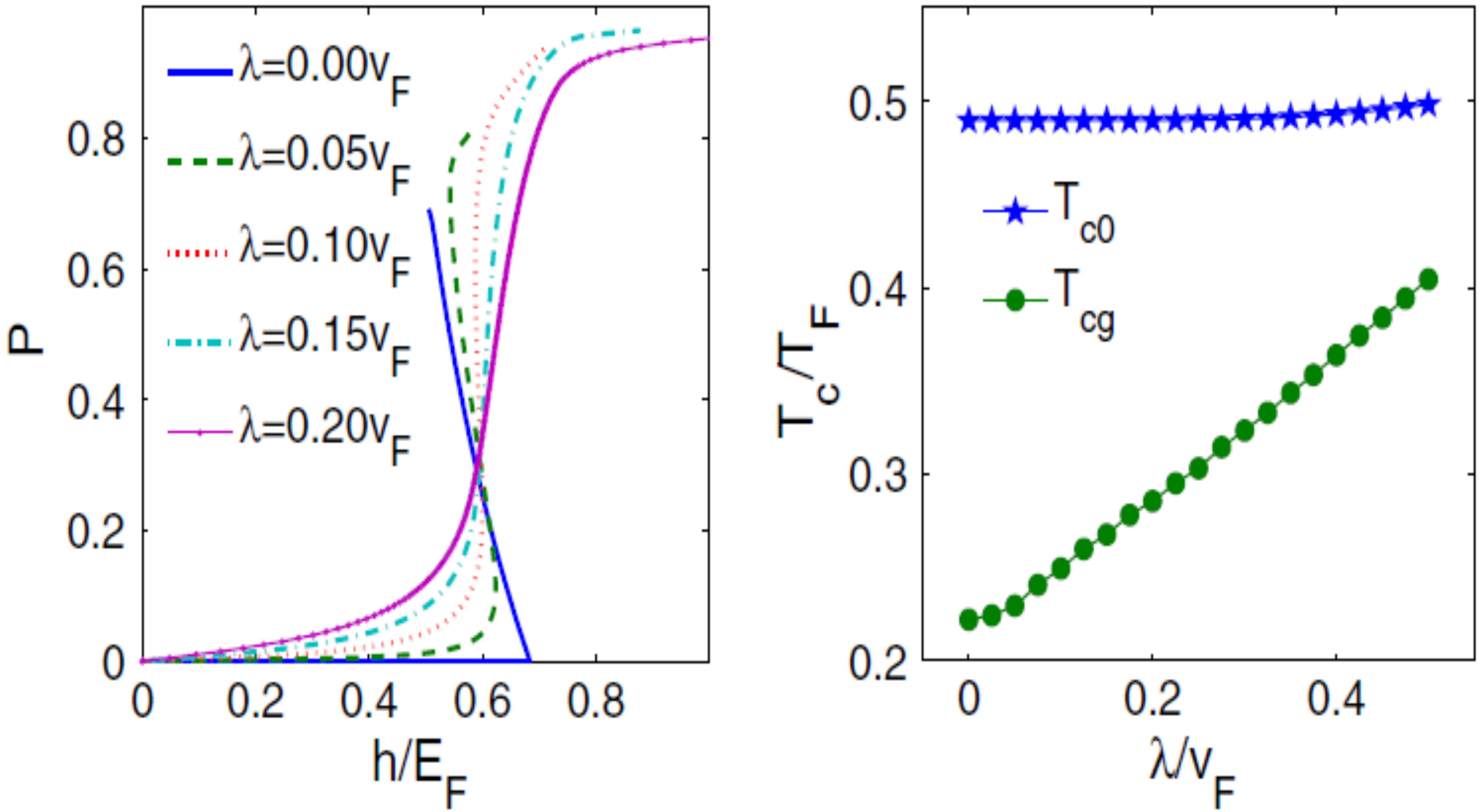

FIG. 4. Left: The polarization P as a function of magnetic field h for various SOC strengthλat zero temperature at unitarity. Right: The critical temperature for balanced superfluid at unitarity; T_{c0} is calculated from mean field theory, T_{cg} is calculated by taking account of Nozieres-Schmitt-Rind correction.

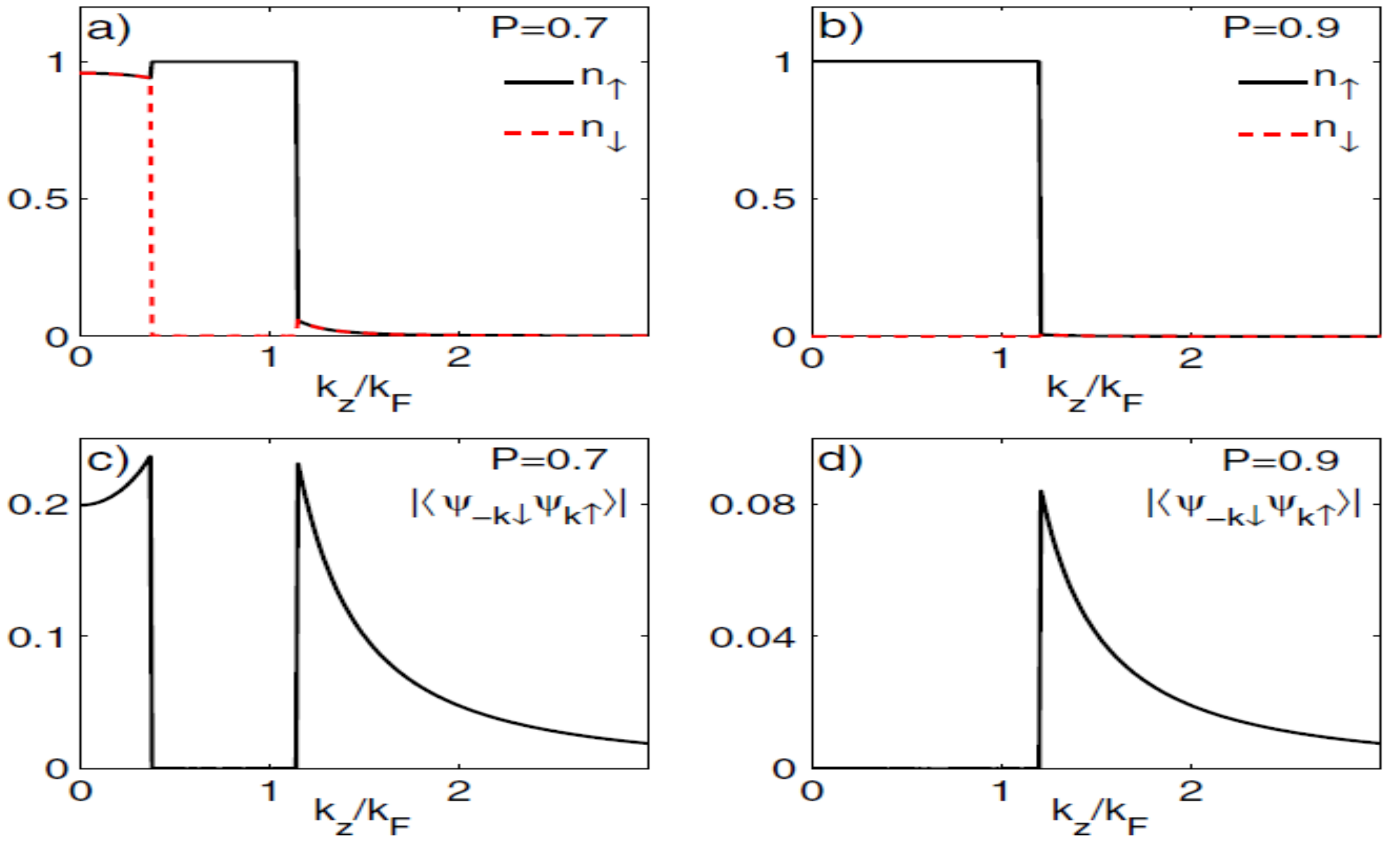

FIG. 5. The momentum distribution $n_{k\sigma}$ and correlation function $C_{\uparrow\downarrow}(k)$ at unitarity at zero temperature with SOC strengthλ=0.2v_F for two typical polarizations: P=0.7 (left) and P=0.9 (right).

6. Higgs in cavity

Y.X. Yu, J.W. Ye, W.M. Liu, Scientific Reports 3, 3476 (2013)

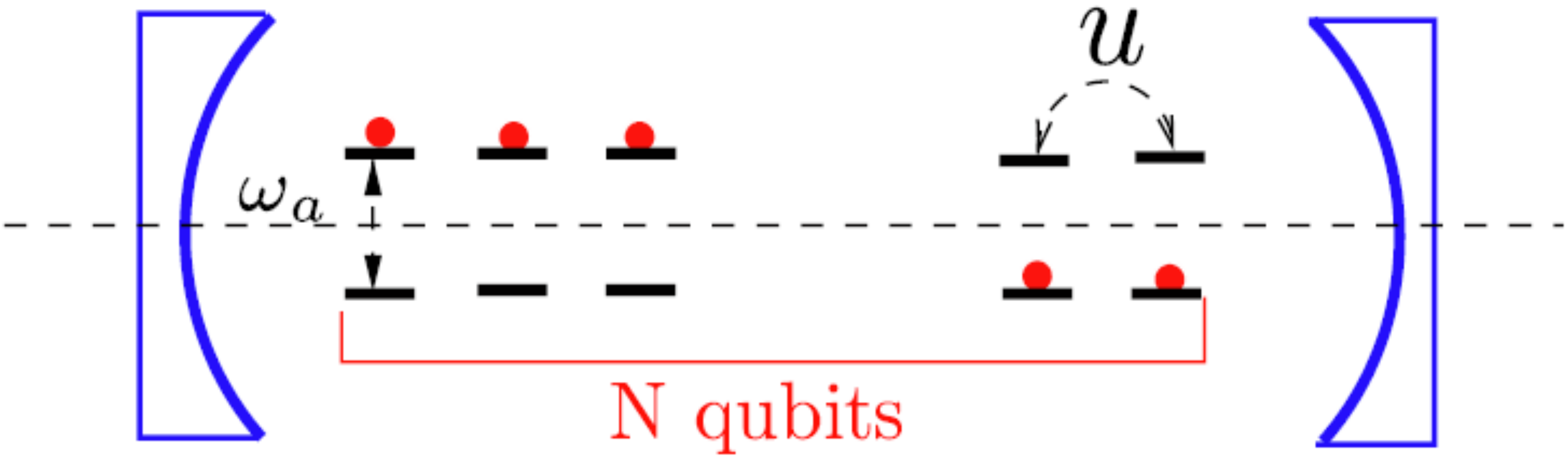

$$H_{U(1)/Z_2} = \omega_a a^\dagger a + \frac{\omega_b}{2}\sum_{i=1}^{N}\sigma_i^z + \frac{g}{\sqrt{N}}\sum_{i=1}^{N}(a^\dagger\sigma_i^- + h.c.)$$

$$+ \frac{g'}{\sqrt{N}}\sum_{i=1}^{N}(a^\dagger\sigma_i^+ + h.c.),$$

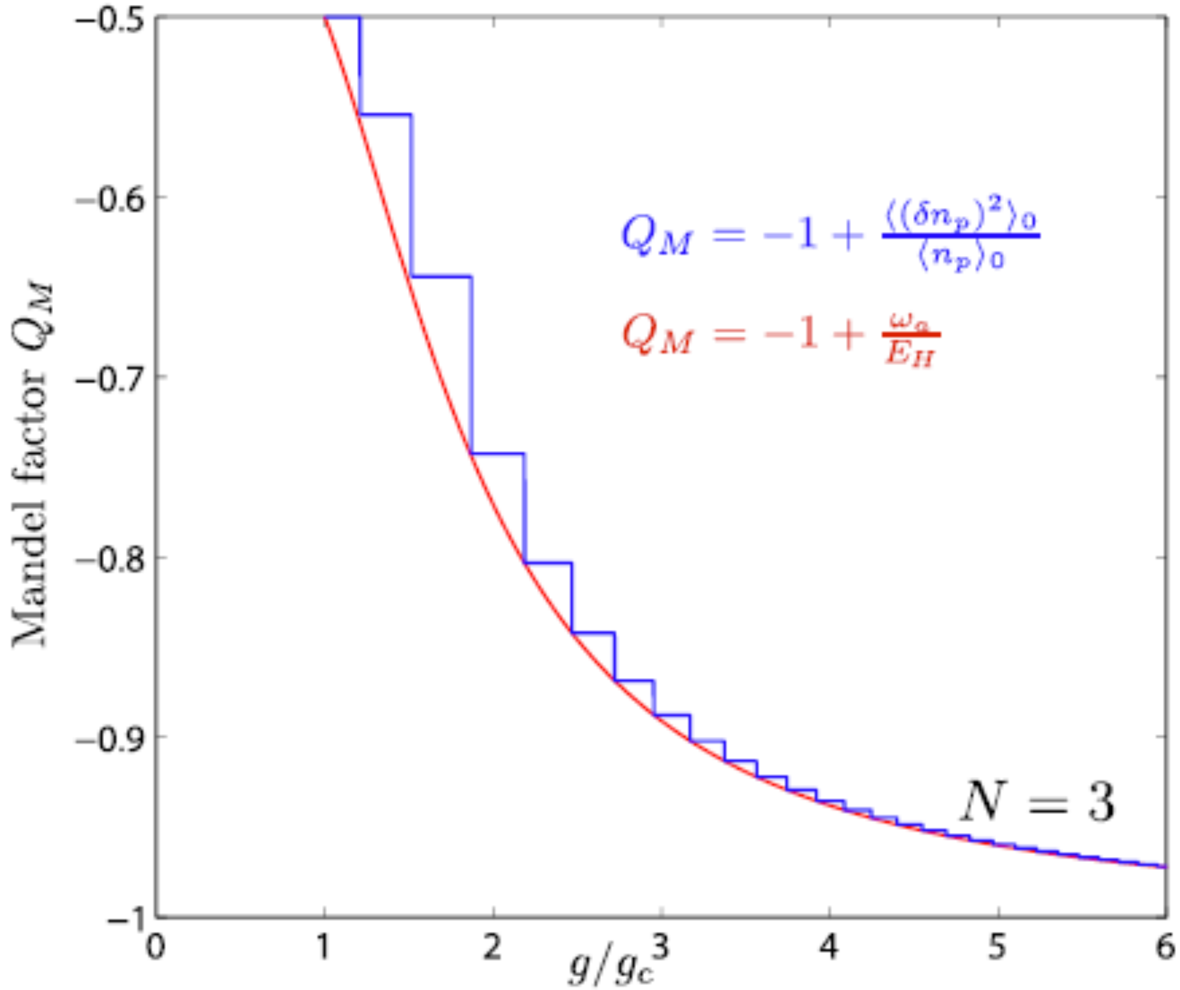

(b)

Figure 1 | (a) N atoms are placed on anti-nodes of a cavity. u is repulsive qubit-qubit interaction which can be tuned to reduce critical coupling g_c. (b) The analytical Mandel factor Q_M (red) against exact diagonalization result (blue) at N=3. It is a number squeezed state inside superradiant phase.

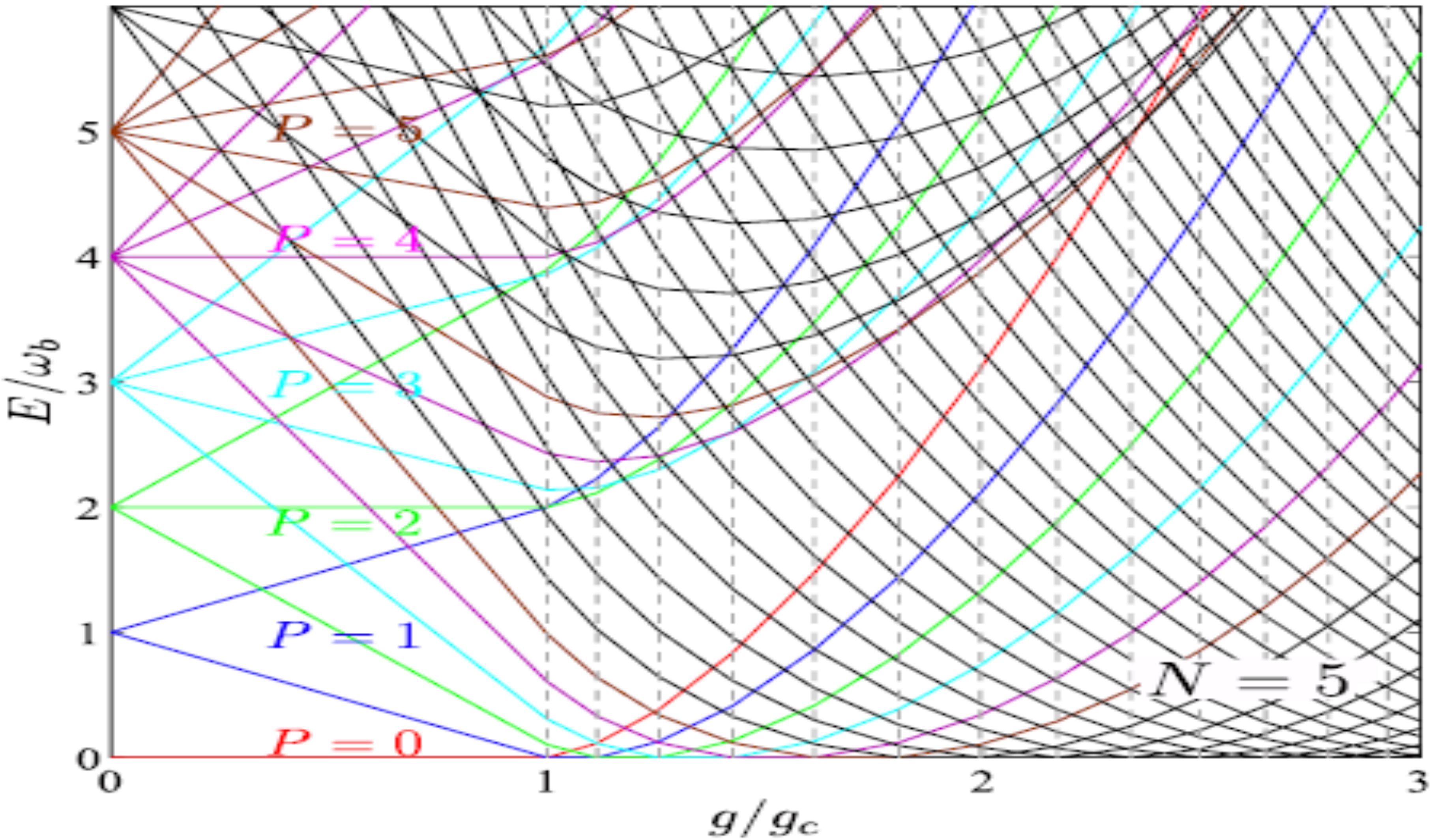

Figure 2 | The exact diagonalization results of energy levels E measured by subtracting ground-state energy versus g/gc at resonance ωa=ω b with N=5 atoms. Different colors of energy curves correspond to several smallest numbers of total excitations number P=a+a + b+b. The dashed vertical lines correspond to critical values of g where number of total excitations P in ground state increases by one.

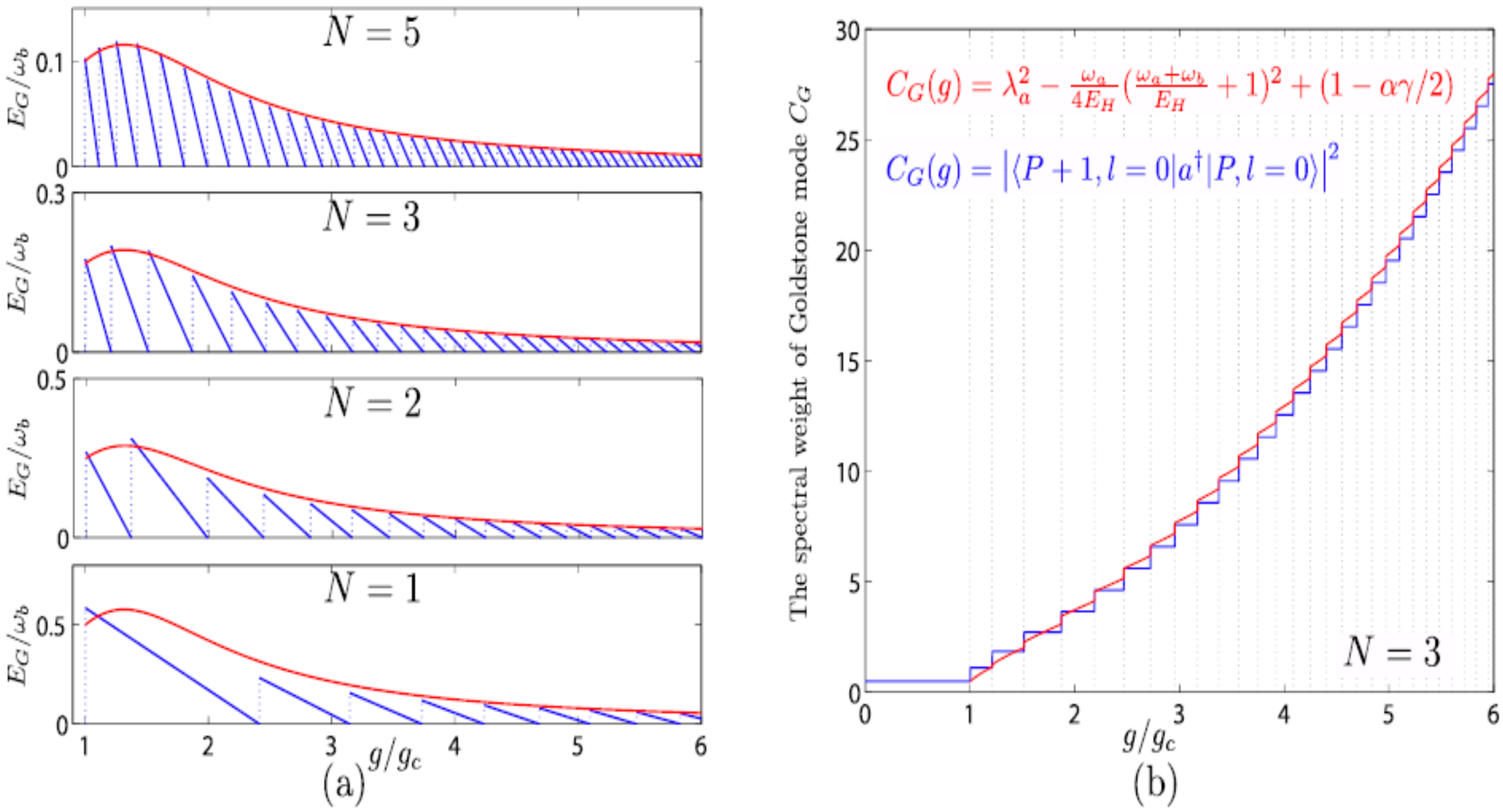

Figure 3 | (a) The analytical Goldstone mode at α=-1/2, $E_G=D(g)=2\omega_a G2/NE_H2$ (red line) are contrasted with ED result $E_G=E_0P+1 - E_0P$ (blue lines) at N=5,3,2,1. It is remarkable that the analytical result can even map out broad peaks at small P in the ED results very precisely. (b) The analytical spectral weight (red) of the Goldstone mode C_G against the ED result (blue) at N=3.

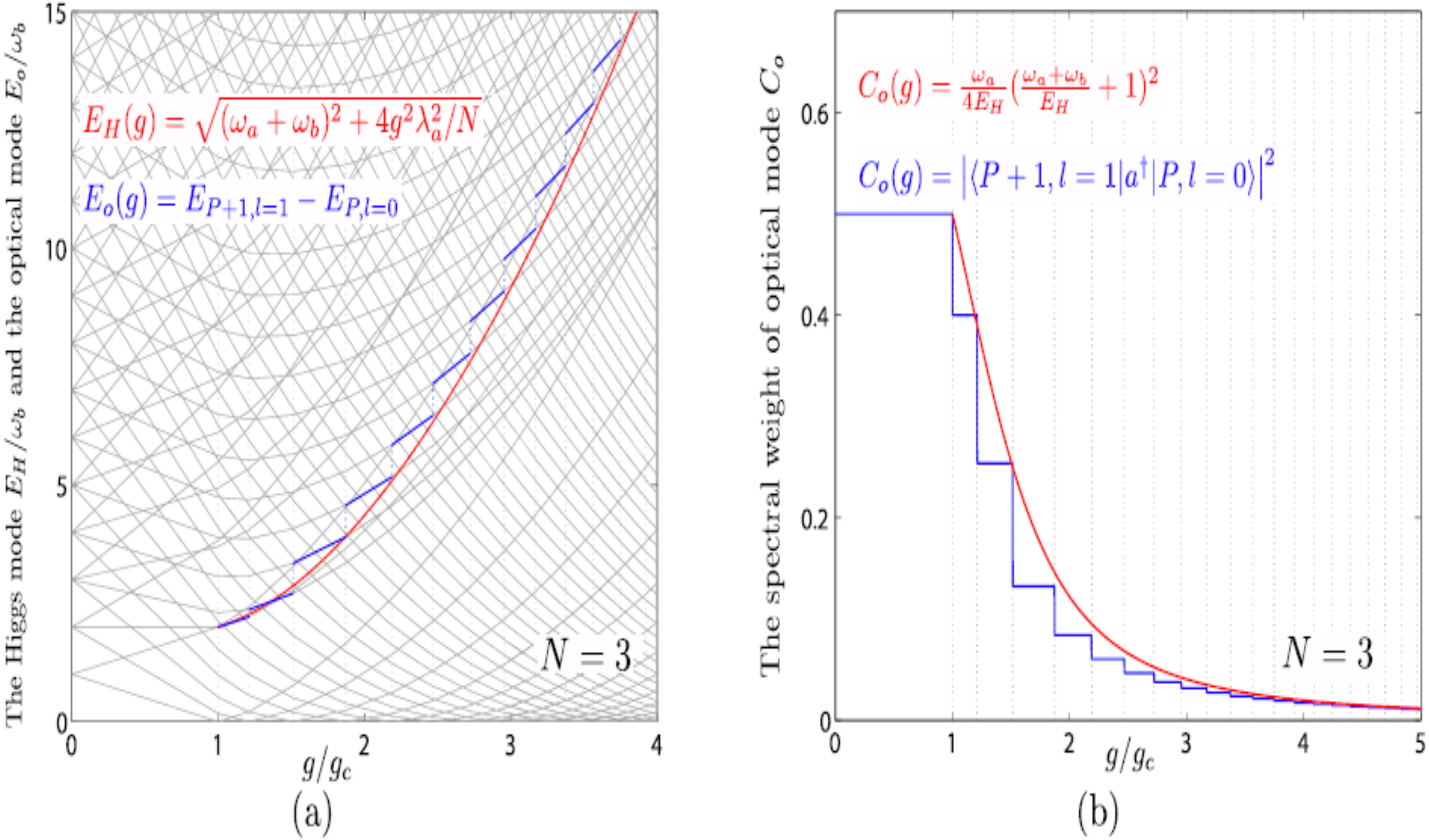

Figure 4 | (a) The analytical relation $E_o=E_H+E_G$ (E_H in red line) is satisfied by ED optical mode $E_o=E_1^{P+1}-E_0^P$ (blue lines) at N=3 except at first few steps. (b) The analytical spectral weight (red) of optical mode C_o against ED result (blue) at N=3.

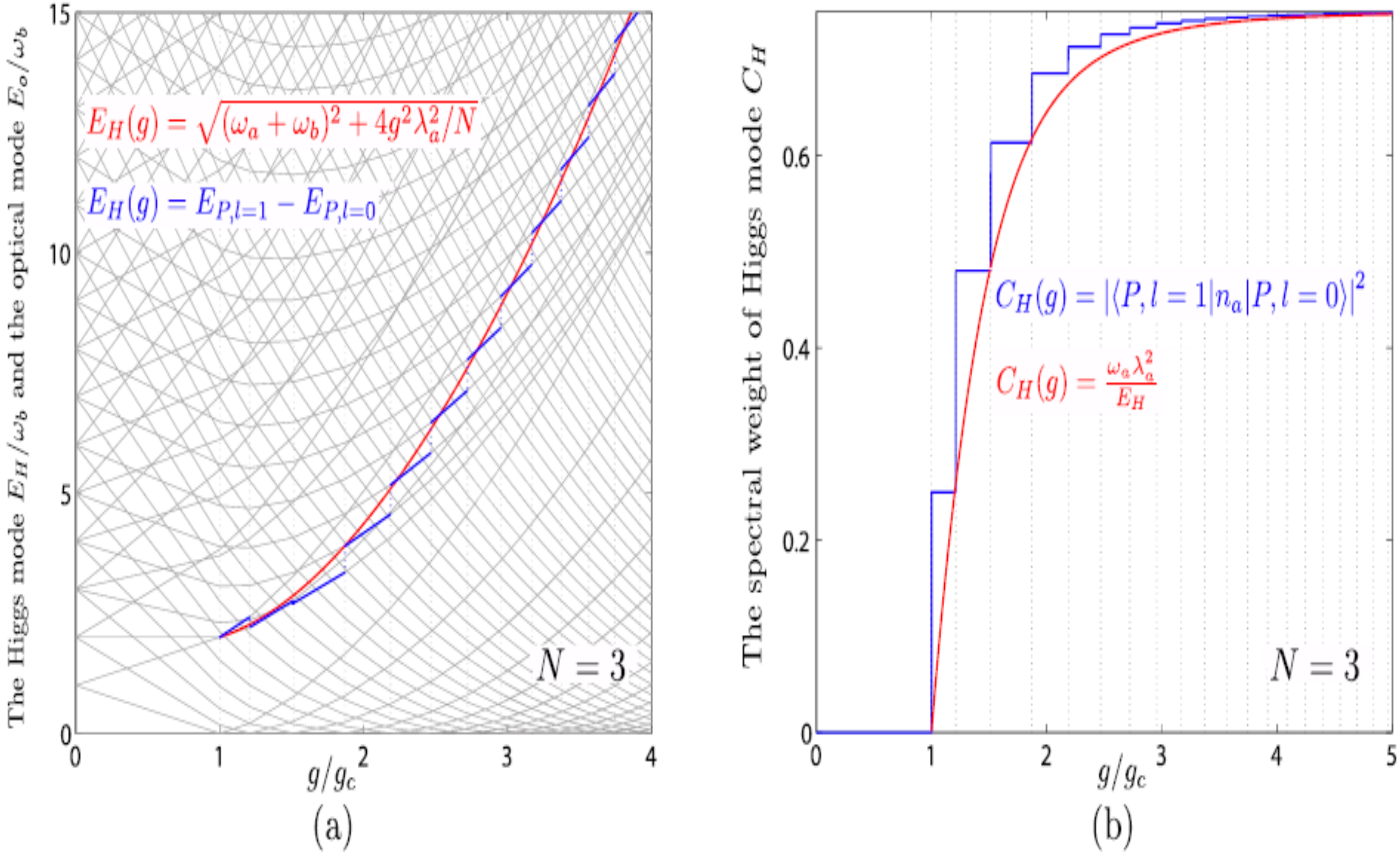

Figure 5 | (a) The analytical Higgs energy EH (red) against exact diagonalization result EH=EP1 - EP0 (blue) at N=3. (b) The analytical spectral spectral weight CH (red) for the Higgs mode against the exact diagonalization result (blue) at N=3.

Summary

1. Higgs in cold atoms
2. Normal state
3. Collective mode
4. Itinerant ferromagnetism
5. Tricritical point
6. Higgs in cavity